Electronic Supplementary Information

A new family of luminescent Iridium Complexes: Synthesis, Optical and Cytotoxic Studies.

Gonzalo Millán,[a] Mattia Nieddu,[a] Icíar P. López,[b] Cintia Ezquerro,[a] Jesús R. Berenguer,[a] Ignacio M. Larráyoz,[c,d] José G. Pichel*[b,e] and Elena Lalinde*[a]

[a] Prof. Dr. E. Lalinde, Dr. J. R. Berenguer, G. Millán, Dr. M. Nieddu, Dr. C. Ezquerro. Departamento de Química-Centro de Síntesis Química de La Rioja, (CISQ), Universidad de La Rioja, 26006, Logroño, Spain. E-mail: elena.lalinde@unirioja.es

[b] Dr. I. P. López, Dr. J. G. Pichel
Lung Cancer and Respiratory Diseases Unit (CIBIR), Fundación Rioja Salud, 26006, Logroño, Spain. E-mail: jgpichel@riojasalud.es

[c] Dr. I.M. Larrayoz
Unidad Predepartamental de Enfermería, Universidad de La Rioja, Duquesa de la Victoria 88, E-26006, Logroño, Spain. E-mail: ignacio.larrayoz@unirioja.es

[d] Dr. I.M. Larrayoz
Biomarkers and Molecular Signaling Unit (CIBIR), Fundación Rioja Salud, 26006, Logroño, Spain

[e] Dr. J. G. Pichel
Biomedical Research Networking Center in Respiratory Diseases (CIBERES), ISCIII, Spain

Contents: Page

1.-Experimental Section

General methods

Complexes have been characterized by elemental analyses, mass spectrometry and the usual spectroscopic means (Ir, Vis/UV, multinuclear NMR). All reactions were carried out under an atmosphere of dry nitrogen, using standard Schlenk techniques. Solvents were obtained from a solvent purification system (M-BRAUN MB SPS-800). Elemental analyses were carried out in a Carlo Erba EA1110 CHNS-O microanalyzer. Mass spectra were recorded by electrospray ionization on an interphase ESI/APCI Bruker Microtof-Q spectrometer with positive and negative ion mode with MeOH/H_2O 90/10 and 0.1 % formic acid as a mobile phase and on a Microflex MALDI-TOF Bruker (MALDI) spectrometer operating in the linear and reflector modes using dithranol as matrix. IR spectra were recorded on a PerkinElmer Spectrum UATR Two FT-IR Spectrometer with the diamond crystal ATR accessory covering the region between 4000 and 450 cm^{-1}; data processing was carried out with Omnic. NMR spectra were recorded on a Bruker AVANCE ARX400 spectrometer at 298 K. Chemical shifts are reported in parts per million (ppm) relative to external standards ($SiMe_4$ for ^1H and $^{13}C\{^1H\}$ and $CFCl_3$ for $^{19}F\{^1H\}$) and coupling constants in Hz. UV-Vis spectra in solution were recorded on an Agilent 8453 spectrophotometer. The excitation and emission spectra as well as lifetime measurements were obtained on an Edinburgh FLS 1000 Fluorescence spectrometer. Lifetimes measurements were performed using a µF2 microsecond lamp flashlamp (Power: 100 W, Fuse: 3.15 Amp A/S) and a Picosecond Pulsed Diode LED with a wavelength of 375 nm with pulse length of 2-20 µs. Quantum yields were measured using a Hamamatsu Absolute PL Quantum Yield Measurement System Spectrometer C11347. Precursors $[Ir(CHO\text{-}dfppy)_2(\mu\text{-}Cl)]_2$ and $([Ir(COOH\text{-}dfppy)_2(\mu\text{-}Cl)]_2$ have been synthesized following similar procedures to those previously established for $[Ir(dfppy)_2(\mu\text{-}Cl)]_2$.[1] C^N ligands {2,6-difluoro-3-(pyridin-2-yl) benzaldehyde (CHO-dfppy)[2] and 2,6- Difluoro-3-pyridin-2-yl-benzoic Acid (COOH-dfppy)[3]} were prepared following previously reported methods. The diimine ligand N,N'-dibutyl-2,2'-bipyridine-4,4'-dicarboxamide (*dbbpy*) was synthetized as previously reported.[4] Other reagents were obtained from commercial sources and used without further purification.

Synthesis of [Ir(CHOdfppy)$_2$(μ-Cl)]$_2$ (1b).

$IrCl_3 \cdot 3H_2O$ (455 mg, 1.27 mmol) was refluxed overnight at 110ºC with 2-fluoro-3-(2-pyridinyl) benzaldehyde (699 mg, 3.18 mmol) in 2- ethoxyethanol and distilled water (3:1). Once the reaction was over, it was cooled to room temperature. A yellow solid precipitated by addition of 30 mL of distilled water, which was filtered and further washed with ethanol and hexane.

Yield: 433 mg (54%).

Anal. Calc. for $C_{48}H_{24}Cl_2F_8Ir_2N_4O_4$: C, 43.41; H, 1.82; N 4.22. Best analyses found: C, 41.78; H, 2.34; N, 3.72, (Elemental analyses fit well for **1b·3H$_2$O**. $C_{48}H_{30}Cl_2F_8Ir_2N_4O_7$: C, 41.71; H, 2.19; N, 4.05). ESI (+): m/z 665.02 $[1/2\ M+H]^+$ (100%). IR (KBr, cm^{-1}): (C-H) 3268 (m), 3057 (m), 2956 (m), 2876 (m); (C=O) 1689 (s); (C-H ring) 1590 (s), 1536 (s), 1426 (m); (C-F) 1294 (m). ^{1}H NMR (400 MHz, $CDCl_3$, δ:) 10.16 (s, CHO); 9.09 (d, $J_{H\text{-}H}$= 5.6 Hz, H^{2}dfppy), 8.46 (d, $J_{H\text{-}H}$= 8.6 Hz, H^{5}dfppy), 8.00 (t, $J_{H\text{-}H}$ = 7.8 Hz, H^{3}dfppy), 6.98 (t, $J_{H\text{-}H}$ = 8.0 Hz, H^{4}dfppy), 5.39 (d, $^3J_{F\text{-}H}$ = 10.6 Hz, H^{9}dfppy). ^{19}F NMR (376.5 MHz, $CDCl_3$) δ -113.03 (d, $J_{F\text{-}F}$ = 7.5 Hz, F^6), -116.52 (d, $J_{F\text{-}F}$ = 7.5 Hz , F^8).

Synthesis of [Ir(COOHdfppy)$_2$(μ-Cl)]$_2$ (1c).

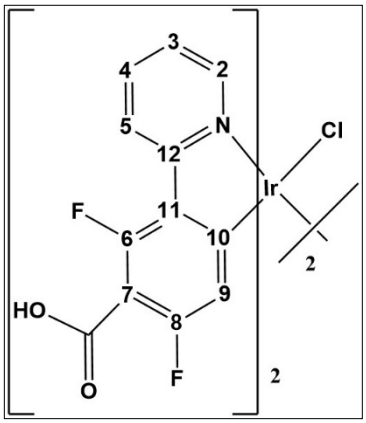

$IrCl_3.3H_2O$ (250 mg, 0.699 mmol) was refluxed for 24 hours at 110ºC with 2-fluoro-3-(2-pyridinyl) benzoic acid (333 mg, 1.398 mmol) in a mixture of 2-ethoxyethanol and distilled water (3:1). After the reaction was completed, the mixture was cooled to room temperature and the solvent evaporated under reduced pressure to obtain a dark oil. **1c** was obtained as a yellow colored precipitate by addition of an aqueous solution of HCl (0,1 M). The solid was filtered and washed with distilled water and diethyl ether. Yield: 320 mg (65%).

ESI (+): m/z 702 $[1/2M\text{-}Cl+Na+H_2O]^+$ (100%), m/z 661 $[1/2M\text{-}Cl]^+$ (38%)). ESI (-): m/z 1391 $[M\text{-}1]^-$ (6%),). MALDI (): m/z 1391 $[M\text{-}1]^-$ (4%), m/z 731 $[1/2M+Cl]^-$ (100%). IR (KBr, cm^{-1}): (N-H) 3385 (m); 2987 (m), 2779 (m); (C=O) 1690 (s); (C-H ring) 1593 (vs), 1539 (s), 1422 (m); (C-F) 1294 (m). ^{1}H NMR (400 MHz, D_2O + KOH, δ:) 8.75 (d, $J_{H\text{-}H}$= 5.6 Hz, H^{2}dfppy), 8.30 (d, $J_{H\text{-}H}$= 8.7 Hz, H^{5}dfppy), 7.96 (t, $J_{H\text{-}H}$ = 7.8 Hz, H^{3}dfppy), 7.45 (t, $J_{H\text{-}H}$ = 7.1 Hz, H^{4}dfppy), 5.64 (d, $^3J_{F\text{-}H}$ = 9.4 Hz, H^{9}dfppy). ^{19}F NMR (376 MHz, D_2O + KOH) δ -113.66 (d, $J_{F\text{-}F}$ = 8.3 Hz, 2F), -115.83 (d, $J_{F\text{-}F}$ = 9.2 Hz, 2F).

Synthesis of [Ir(dfppy)$_2$(dbbpy)]Cl (2a-Cl).

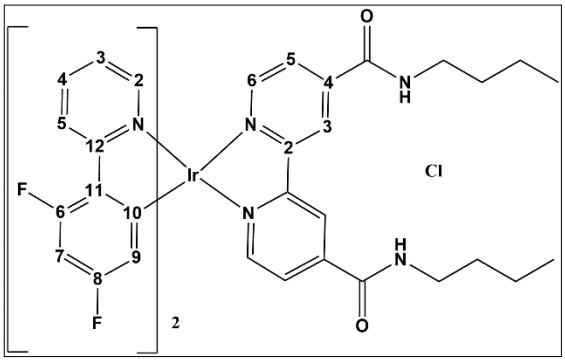

250 mg (0.21 mmol) of [Ir(dfppy)$_2$(μ-Cl)]$_2$ and 180 mg (0.49 mmol) of *dbbpy* were refluxed under N_2 atmosphere in a mixture of methanol and CH_2Cl_2 (1:2 v/v) for 12 hours. After cooling, the solution was concentrated to 2 ml with a rotary evaporator. Then the addition of diethyl ether yields **2a-Cl** as a yellow solid (270 mg, 70%).

ESI (+): m/z 927 $[M]^+$ (100%). IR (KBr, cm^{-1}): (N-H) 3427 (m); (C-H) 3297 (m), 3240 (m), 3060 (m), 2956 (m), 2920 (m), 2863 (m); (C=O) 1660 (s); (C-H ring) 1603 (vs), 1570 (s), 1553 (s), 1473 (s), 1426 (m), 1403 (s); (C-F) 1286 (m).^{1}H NMR (400 MHz, $CDCl_3$, δ): 10.66 (s, H^{3}dbbpy); 9.63 (s br, NH); 8.35 (d, J_{H-H} = 8.5 Hz, H^{2}dfppy); 8.18 (d, J_{H-H} = 5.7 Hz, H^{6}dbbpy or H^{5}dbbpy); 8.00 (d, J_{H-H} = 5.7 Hz, H^{6}dbbpy or H^{5}dbbpy); 7.85 (t, J_{H-H} = 8.1 Hz, H^{3}dfppy); 7.40 (d, J_{H-H} = 5.9 Hz, H^{5}dfppy); 7.03 (t, J_{H-H} = 6.8 Hz, H^{4}dfppy); 6.60 (pst, $3J_{F-H}$ = 10.7 Hz, H^{7}dfppy); 5.69 (dd, $^3J_{F-H}$ = 8.2 Hz, J_{H-H} = 2.3 Hz, H^{9}dfppy); 3.56 (c, J_{H-H} = 7.0 Hz, 2H, $NHCH_2$); 1.77 (q, J_{H-H} = 7.5 Hz, 2H, $NHCH_2CH_2$); 1.43 (sx, J_{H-H} = 7.5 Hz, 2H, CH_2CH_3); 0.94 (t, JH-H = 7.3 Hz, 3H, $CH_2CH_2CH_2CH_3$). ^{13}C{^{1}H} NMR (100.6 MHz, $CDCl_3$, δ): 164.6 (s, C^{12}dfppy); 161.8 (s, CO); 161.6 (dd, J_{F-C} = 232 Hz, $^3J_{F-C}$ = 13 Hz, C^{6}dfppy or C^{8}dfppy); 156.4 (s, C^{4}dbbpy or C^{2}dbbpy); 153.2 (m, C^{10}dfppy or C^{11}dfppy); 150.4 (s, C^{6}dbbpy or C^{5}bdbbpy); 148.3 (s, C^{5}dfppy); 145.2 (s, C^{4}dbbpy or C^{2}dbbpy); 139.0 (s, C^{3}dfppy); 128.1 (s, C^{6}dbbpy or C^{5}dbbpy); 127.6 (d, J_{F-C} = 280 Hz, C^{6}dfppy or C^{8}dfppy); 127.5 (C^{10}dfppy or C^{11}dfppy); 124.3 (s, C^{2}dfppy or C^{3}dbbpy); 124.1 (s, C^{2}dfppy or C^{3}dbbpy); 123.7 (s, C^{4}dfppy); 114.2 (d, $^2J_{F-C}$ ≈ 20 Hz, C^{9}dfppy); 99.8 (pst, $^2J_{F-C}$ ≈ 28 Hz, C^{7}dfppy); 40.7 (s, $NHCH_2$); 31.5 (s, $NHCH_2CH_2$); 20.5 (s, CH_2CH_3); 14.0 (s, CH_3). ^{19}F{^{1}H} NMR (376.5 MHz, $CDCl_3$, δ): -104.71 (d, J_{F-F} = 11.5 Hz, 2F, F^6); -107.86 (d, J_{F-F} = 11.5 Hz, 2F, F^8).

Synthesis of [Ir(CHOdfppy)$_2$(dbbpy)]Cl (2b-Cl).

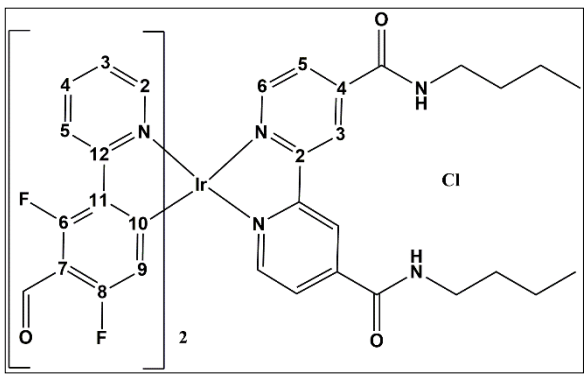

This compound was obtained as an orange solid (160 mg, 88%) following a similar procedure to that described for **2a**. By using *dbbpy* (80 mg, 0.22 mmol) and

$[Ir(CHOdfppy)_2(\mu\text{-}Cl)]_2$ (110 mg, 0.09 mmol) as precursors.

ESI (+): m/z 983 $[M]^+$ (100%). IR (KBr, cm^{-1}): (N-H) 3437 (m); (C-H) 3300 (m), 3216 (m), 3060 (m), 2956 (m), 2935 (m), 2867 (m); (C=O) 1690 (s); (C-H ring) 1632 (vs), 1594 (s), 1530 (s), 1471 (s), 1423 (m), 1354 (s); (C-F) 1231 (m).^{1}H NMR (400 MHz, $CDCl_3$, δ): 10.56 (s, br, H^3dbbpy); 10.30 (s, CHO); 9.53 (s br, NH); 8.48 (d, $J_{H\text{-}H}$ = 8.5 Hz, H^2dfppy); 8.22 (d, $J_{H\text{-}H}$ = 5.5 Hz, H^6dbbpy); 7.98 (m, 2H, H^5dbbpy and H^3dfppy); 7.47 (d, $J_{H\text{-}H}$ = 5.5 Hz, H^5dfppy); 7.19 (t, $J_{H\text{-}H}$ = 6.3 Hz, H^4dfppy); 5.84 (d, $^3J_{F\text{-}H}$ = 9.5 Hz, H^9dfppy); 3.54 (m, 2H, $NHCH_2$); 1.74 (q, $J_{H\text{-}H}$ = 7.5 Hz, 2H, $NHCH_2CH_2$); 1.43 (sx, $J_{H\text{-}H}$ = 7.5 Hz, 2H, CH_2CH_3); 0.96 (t, $J_{H\text{-}H}$ = 7.3 Hz, 3H, CH_3). $^{13}C\{^1H\}$ NMR (100.6 MHz, $CDCl_3$, δ): 183.9 (t, $J_{F\text{-}C}$ = 5 Hz, CHO); 165 – 159 (m, 4C, C^6dfppy, C^8dfppy, C^{12}dfppy and C^{11}dfppy); 161.60 (s, CO); 156.1 (s, C^4dbbpy or C^2dbbpy); 150.3 (s, C^5dbbpy); 148.7 (s, C^5dfppy); 146.1 (s, C^4dbbpy or C^2dbbpy); 140.5 (s, C^3dfppy); 128.5 (s, C^6dbbpy); 128.4 (s, C^{10}dfppy); 125.2 (s, C^3dbbpy); 125.0 (s, C^2dfppy); 124.5 (s, C^4dfppy); 115.3 (d, $J_{F\text{-}C}$ = 18 Hz, C^9dfppy); 110.7 (t, $J_{F\text{-}C}$ = 11 Hz C^7dfppy); 40.7 (s, $NHCH_2$); 31.4 (s, $NHCH_2CH_2$); 20.5 (s, CH_2CH_3); 13.9 (s, CH_3). $^{19}F\{^1H\}$ NMR (376.5 MHz, $CDCl_3$, δ): -110.47 (d, $J_{F\text{-}F}$ = 7.9 Hz, 2F, F^6); -114.57 (d, $J_{F\text{-}F}$ = 7.6 Hz, 2F, F^8).

Synthesis of $[Ir(CHOdfppy)_2(dbbpy)]PF_6$ (2b-PF_6).

This compound was synthesized as an orange solid by the addition of 2 equiv. (100 mg, 0.28 mmol.) of $TlPF_6$ to a solution of (**1b**) $Ir(CHOdfppy)_2(\mu\text{-}Cl)]_2$ (177 mg, 0.14 mmol.) in 10 ml of anhydrous acetonitrile. The suspension was refluxed 2 hours and then was filtered through celite. The resulting solution was evaporated to dryness to give $[Ir(CHOdfppy)_2(NCMe)_2]PF_6$ as a yellow solid. The solid was redissolved in 10 ml of anhydrous CH_2Cl_2 and the yellow solution treated with a solution of *dbbpy* (100 mg, 0.28 mmol) in 20 ml of distilled methanol (20 ml) was refluxed for 48 hours and finally evaporated to dryness to give **2b-PF_6** as an orange solid which was filtered and washed with diethylether.

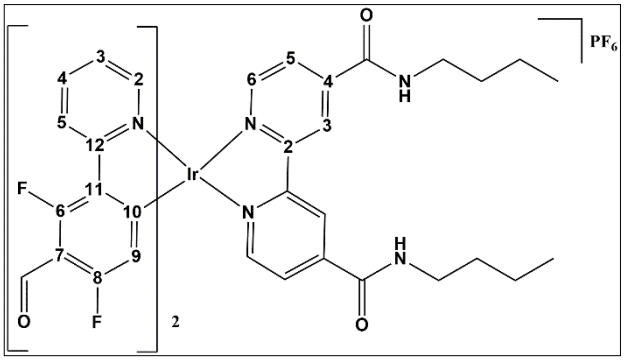

ESI (+): m/z 983 $[M]^+$ (100%). IR (KBr, cm^{-1}): (N-H) 3285 (m); (C-H) 2932 (m), 2866 (m); (C=O) 1700 (s); (C-H ring) 1600 (vs), 1545 (s), 1528 (s), 1473 (s); (C-F) 1235 (m); ν(P-F) 838 (m). ^{1}H NMR (400 MHz, $CDCl_3$, δ): 10.44 (s, br, H^3dbbpy); 10.30 (s, CHO);

9.36 (s br, NH); 8.47 (d, J_{H-H} = 8.6 Hz, H^2dfppy); 8.21 (d, J_{H-H} = 5.6 Hz, H^6dbbpy); 7.99 (t, J_{H-H} = 7.5 Hz, H^3dfppy); 7.98 (d, J_{H-H} = 5.7Hz, H^5dbbpy); 7.47 (d, J_{H-H} = 5.6 Hz, H^5dfppy); 7.19 (t, J_{H-H} = 6.6 Hz, H^4dfppy); 5.83 (d, $^3J_{F-H}$ = 9.8 Hz, H^9dfppy); 3.56 (m, 2H, $NHCH_2$); 1.76 (q, J_{H-H} = 7.5 Hz, 2H, $NHCH_2CH_2$); 1.42 (m, , 2H, CH_2CH_3); 0.95 (t, J_{H-H} = 7.4 Hz, 3H, CH_3). $^{13}C\{^1H\}$ NMR (100.6 MHz, $CDCl_3$, δ): 184.0 (t, J_{F-C} = 6 Hz, CHO); 165 – 159 (m, 4C, C^6dfppy, C^8dfppy, C^{12}dfppy and C^{11}dfppy); 162.11 (s, CO); 156.1 (s, C^4dbbpy or C^2dbbpy); 150.4 (s, C^5dbbpy or C^3dfppy); 148.8 (s, C^5dfppy); 146.3 (s, C^4dbbpy or C^2dbbpy); 140.5 (s, C^5dbbpy or C^3dfppy); 128.6 (s, C^6dbbpy); 128.4 (s, C^{10}dfppy); 125.1 (s, C^4dbbpy); 125.0 (s, C^2dfppy); 124.3 (s, C^3dbbpy); 115.2 (d, J_{F-C} = 16 Hz, C^9dfppy); 110.7 (m, C^7dfppy); 40.8 (s, $NHCH_2$); 31.4 (s, $NHCH_2CH_2$); 20.5 (s, CH_2CH_3); 13.9 (s, CH_3). $^{19}F\{^1H\}$ NMR (376.5 MHz, $CDCl_3$, δ): -71.25 (d, J_{P-F} = 715 Hz, PF_6); -110.49 (d, J_{F-F} = 7.8 Hz, 2F, F^6); -114.59 (d, J_{F-F} = 7.6 Hz, 2F, F^8). $^{31}P\{^1H\}$ NMR (162.1 MHz, $(CD_3)_2CO$, δ): -144.3 (sp, J_{P-F} = 708.0 Hz, PF_6).

Synthesis of [Ir(COOHdfppy)$_2$(dbbpy)]Cl (2c-Cl).

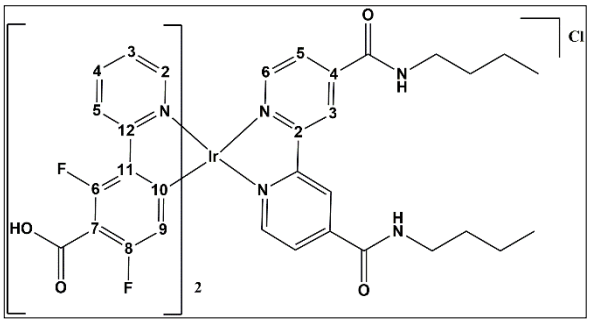

This compound was obtained as an orange solid (80 mg, 54%) following a procedure similar to that described for **2b-Cl,** using *dbbpy* (56 mg, 0.158 mmol) and Ir(COOHdfppy)$_2$(μ-Cl)]$_2$ (100 g, 0.08 mmol) as starting precursors. These precursors were refluxed for 6 hours in a mixture of methanol and CH_2Cl_2 (1:2 v/v), under nitrogen conditions. The solution was cooled, concentrated, and finally precipitated with diethyl ether.

ESI (+): m/z 1015.21 $[M]^+$ (100%). IR (KBr, cm^{-1}): (N-H) 3302 (m); (C-H) 3054 (m), 2956 (m), 2867 (m); (C=O) 1600 (s); (C-F) 1293 (m).^{1}H NMR (400 MHz, MeOD, δ): 9.21 (s, H^3dbbpy); 8.37 (d, J_{H-H} = 8.5 Hz, H^2dfppy); 8.17 (d, J_{H-H} = 5.6 Hz, H^6dbbpy); 7.98 (d, J_{H-H} = 5.6 Hz, H^5dbbpy); 7.96 (t, J_{H-H} = 8.5 Hz, H^3dfppy); 7.70 (d, J_{H-H} = 5.7 Hz, H^5dfppy); 7.14 (t, J_{H-H} = 6.5 Hz, H^4dfppy); 5.66 (d, $^3J_{F-H}$ = 8.5 Hz, H^9dfppy); 3.44 (t, J_{H-H} = 7.2 Hz, 2H, $NHCH_2$); 1.64 (q, J_{H-H} = 7.4 Hz, 2H, $NHCH_2CH_2$); 1.42 (m, J_{H-H} = 7.6 Hz, 2H, CH_2CH_3); 0.97 (t, J_{H-H} = 7.2 Hz, 3H, CH_3). $^{13}C\{^1H\}$ NMR (100.6 MHz, MeOD, δ): 168.92 (s, COOH); 165.53 (s, CONH); 165.42 (s, C^{12}); 161.13 (dd, J_{F-C} = 258, $^3J_{F-C}$ = 10 Hz, C^6dfppy or C^8dfppy); 159.10 (dd, J_{F-C} = 258, $^3J_{F-C}$ = 10 Hz, C^6dfppy or C^8dfppy); 157.55 (s, C^4dbbpy or C^2dbbpy); 152.33 (s, C^6dbbpy); 150.68 (s, C^5dfppy); 147.41 (s,

C^4dbbpy or C^2dbbpy); 140.91 (s, C^3dfppy); 128.68 (d, J_{F-C} = 3.8 Hz ,C^{10}dfppy); 127.82 (s, C^5dbbpy); 125.18 (s, C^4dfppy); 124.91 (d, J_{F-C} = 19.8 Hz, C^{11}dfppy);) 124.46 (s, C^2dfppy); 120.18 (s, C^3dbbpy); 116.13 (t, J_{F-C} = 27.3 Hz ,C^7dfppy); 114.70 (d, J_{F-C} = 19.0 Hz ,C^9dfppy); 41.9 (s, $NHCH_2$); 32.64 (s, $NHCH_2CH_2$); 21.34 (s, CH_2CH_3); 14.23 (s, CH_3). $^{19}F\{^1H\}$ NMR (376.5 MHz, MeOD, δ): -114.73 (d, J_{F-F} = 10.0 Hz, F^8), -118.7 (d, J_{F-F} = 10.0 Hz, F^6).

Synthesis of $[Ir(COOHdfppy)_2(dbbpy)]PF_6$ (2c-PF_6).

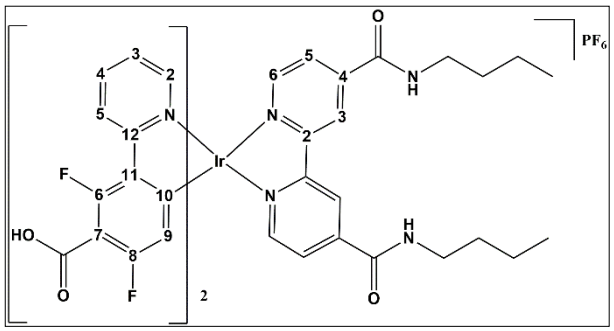

This compound was synthesized as an orange solid following a similiar procedure to that employed for the shynthesis of complexe **2b-PF_6**. 2 equivalents 100 mg, (0.28 mmol.) of $TlPF_6$ were added to a solution of (**1c**) $Ir(COOHdFppy)_2(\mu\text{-}Cl)]_2$ (123 mg, 0.14 mmol.) in 10 ml of anhydrous acetonitrile. The suspension was refluxed 2 hours and lately, when the reaction was completed, the TlCl was filtered through celite. Evaporation of the solvent gives $[Ir(CHOdFppy)_2(NCMe)_2]PF_6$ as a yellow solid. The solid was redissolved in CH_2Cl_2 (10 ml) and treated with a solution of *dbbpy* (95 mg, 0.28 mmol) in distilled methanol (20 ml). The mixture was refluxed 48 hours and finally evaporated to dryness to give **2c-PF_6** as an orange solid which was filtered and washed with diethylether.

ESI (+): m/z 1015.21 $[M]^+$ (100%). IR (KBr, cm^{-1}): (N-H) 3440 (m); (C-H) 3058 (m), 2950 (m), 2866 (m); (C=O) 1700 (s); (C-H ring) 1605 (vs), 1527 (s), 1411 (s); (C-F) 1235 (m); ν(P-F) 819 (vs). ^1H NMR (400 MHz, $(CD_3)_2CO$, δ): 9.20 (s, H^3bpy); 8.47 (m, H^2dfppy and H^5dbbpy or H^6dbbpy); 8.34 (t, J_{H-H} = 6.5 Hz, NH); 8.12 (t, J_{H-H} = 8.4 Hz, H^3dfppy); 8.10 (d, J_{H-H} = 6.4 Hz H^5dbbpy or H^6dbbpy); 8.03 (d, J_{H-H} = 5.8 Hz, H^5dfppy); 7.29 (t, J_{H-H} = 6.6 Hz, H^4dfppy); 5.90 (d, $^3J_{F-H}$ = 9.4 Hz, H^9dfppy); 3.45 (q, J_{H-H} = 7.4 Hz, 2H, $NHCH_2$); 1.59 (q, J_{H-H} = 7.5 Hz, 2H, $NHCH_2CH_2$); 1.38 (sx, J_{H-H} = 7.5 Hz, 2H, CH_2CH_3); 0.92 (t, J_{H-H} = 7.5 Hz, 3H, CH_3). $^{13}C\{^1H\}$ NMR (100.6 MHz, $(CD_3)_2CO$, δ): 163.54 (s, CONH); 164.13 (s, C^{12}); 162.65(s, COOH); 162.61 (dd, J_{F-C} = 288, $^3J_{F-C}$ = 10 Hz, C^6dfppy or C^8dfppy); 159.06 (dd, J_{F-C} = 237, $^3J_{F-C}$ = 8 Hz, C^6dfppy or C^8dfppy); 157.06 (s, C^2dbbpy or C^4dbbpy); 153.02(s, C^5dbbpy or C^6bpy); 151.08 (s, C^5dfppy); 146.35 (s, C^2dbbpy or C^4dbbpy); 141.21 (s, C^3dfppy); 127.65 (s, C^5dbbpy or C^6dbbpy); 125.76 (s, C^4dfppy); 125.20 (d, J_{F-C} = 21, C^2dfppy); 125.20 (d, J_{F-C} = 21, C^2dfppy); 124.48

(t, J_{F-C} = 15.0 Hz ,C^7dfppy); 123.99 (s, C^3dbbpy); 115.30 (t, J_{F-C} = 19.1 Hz ,C^9dFppy); 40.60 (s, $NHCH_2$); 32.19 (s, $NHCH_2CH_2$); 19.93 (s, CH_2CH_3); 14.01 (s, CH_3). -72.6 (d, J_{F-F} = 707.7 Hz, PF_6); -108. 47 (d, J_{F-C} = 6.8 Hz ,C^{10}dfppy); -11.61 (d, J_{F-C} = 6.8 Hz, C^{11}dfppy);) $^{19}F\{^1H\}$ NMR (376.5 MHz, $(CD_3)_2CO$, δ): -72.6 (d, J_{P-F} = 707.7 Hz, PF_6); -108.5 (d, J_{F-F} = 7.0 Hz, F^6); -116.6(d, J_{F-F} = 7.0 Hz, F^8). $^{31}P\{^1H\}$ NMR (162.1 MHz, $(CD_3)_2CO$, δ): -144.3 (sp, J_{P-F} = 708.0 Hz, PF_6).

Synthesis of [Ir(dfppy)$_2$(3,3′-H$_2$dcbpy)]PF$_6$ (3a-PF$_6$).

A yellow solution of 0.25 g (0.21 mmol) of $[Ir(dFppy)_2(\mu\text{-}Cl)]_2$ in CH_2Cl_2 (20 ml) was treated with a solution of 100 mg (0.42 mmol) of 2,2′-bipyridin-3,3′-dicarboxylic acid (3,3′-H_2dcbpy) in methanol (20 ml) and the mixture was refluxed for 2 hours. Then, 5 ml of a saturated solution of NaAcO in MeOH were added and the mixture was refluxed again for 1 hour. A saturated solution of NH_4PF_6 in methanol (5 ml) was added to the mixture and stirred for 30 minutes. The resulting solution was evaporated to dryness and the residue treated with 20 ml of HCl (1M) and stirred for 10 minutes. The yellow solid obtained was filtered, washed with water (2 x 10 ml) and extracted with methanol. The solution was treated with 5 ml of a saturated solution of NH_4PF_6 in methanol and the mixture further stirred for 30 min. and solvent evaporation under reduced pressure gives **3a-PF$_6$** as yellow solid (260 mg, 65%).

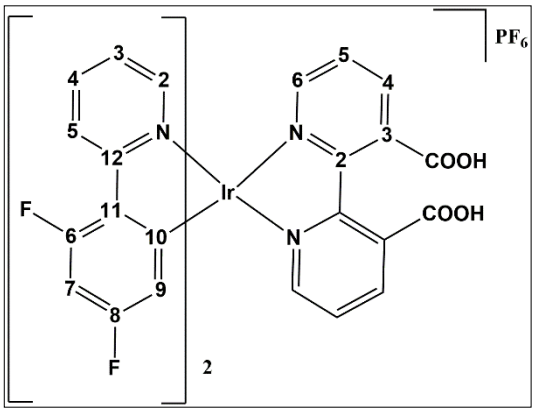

ESI (+): m/z 817 $[M]^+$ (100%). IR (KBr, cm^{-1}): (N-H) 3400 (s, broad); (C-H) 3070 (m), (C=O) 1716 (s); (C-H ring) 1602 (vs), 1569 (s), 1542 (s), 1471 (s), 1393 (s); (C-F) 1242 (m).^{1}H NMR (400 MHz, $(CD_3)_2CO$, δ): 8.54 (d, J_{H-H} = 7.9 Hz, H^6dcbpy); 8.38 (d, J_{H-H} = 8.5 Hz, H^2dfppy); 8.35 (s, br, H^4dcbpy); 8.33 (d, J_{H-H} = 5.2 Hz, H^5dFppy); 8.08 (t, J_{H-H} = 7.9 Hz, H^3dfppy); 7.75 (s, br, H^5dcbpy); 7.31(t, J_{H-H} = 7.0 Hz, H^4dfppy); 6.77 (ddd, $^3J_{F-H}$ = 12 Hz$^3J_{F-H}$ = 12.5 Hz$^3J_{F-H}$ = 2.2 Hz, H^7dfppy); 5.76(dd, J_{F-H} = 8.7 Hz, J_{H-H} = 2.2 Hz, H^9dfppy); $^{13}C\{^1H$ NMR (100.6 MHz, $(CD_3)_2CO$, δ): 164.6 (dd, J_{F-C} = 219, $^3J_{F-C}$ = 12 Hz, C^6dfppy or C^8dfppy); 162.0 (dd, J_{F-C} = 219, $^3J_{F-C}$ = 12 Hz, C^6dfppy or C^8dfppy); 157.0 (s, C^2dcbpy or C^3dcbpy or COOH); 152.6 (s, C^5dfppy); 150.7 (d, J_{F-C} = 7 Hz, C^{12}dfppy) 140.0 (s, C^3dfppy); 140.7 (s, C^6dcbpy); 128.9 (m, C^{10}dfppy and C^{11}dfppy); 128.8 (s, C^5cdbpy); 125.1 (s, C^4dfppy); 124.7 (s, C^4dcbpy); 124.5 (s, C^2dfppy); 114.8 (d, J_{F-C} =

18 Hz, C^9dfppy); 99.9 (t, J_{F-C} = 27 Hz C^7dfppy); $^{19}F\{^1H\}$ NMR (376.5 MHz, $(CD_3)_2CO$, δ): -72.6 (d, J_{P-F} = 707.7 Hz, PF_6); -107.5 (d, J_{F-F} = 10.0 Hz, F^6); -109.9 (d, J_{F-F} = 10.0 Hz, F^8). $^{31}P\{^1H\}$ NMR (162.1 MHz, $(CD_3)_2CO$, δ): -144.3 (sp, J_{P-F} = 710.0 Hz, PF_6).

2.- NMR Spectra

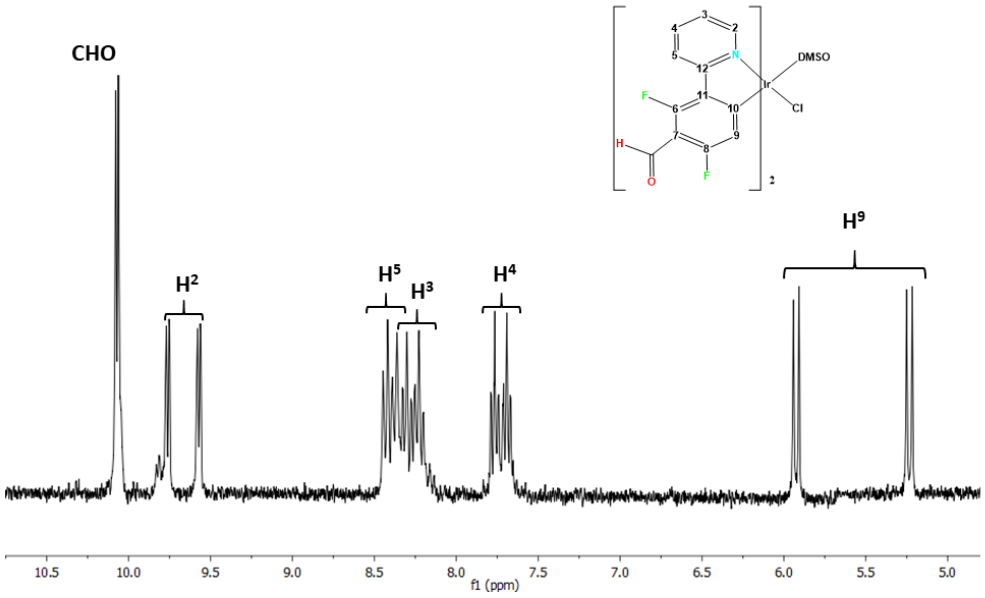

Figure S1.1. NMR ^{1}H spectra of **1b** in d_6- DMSO.

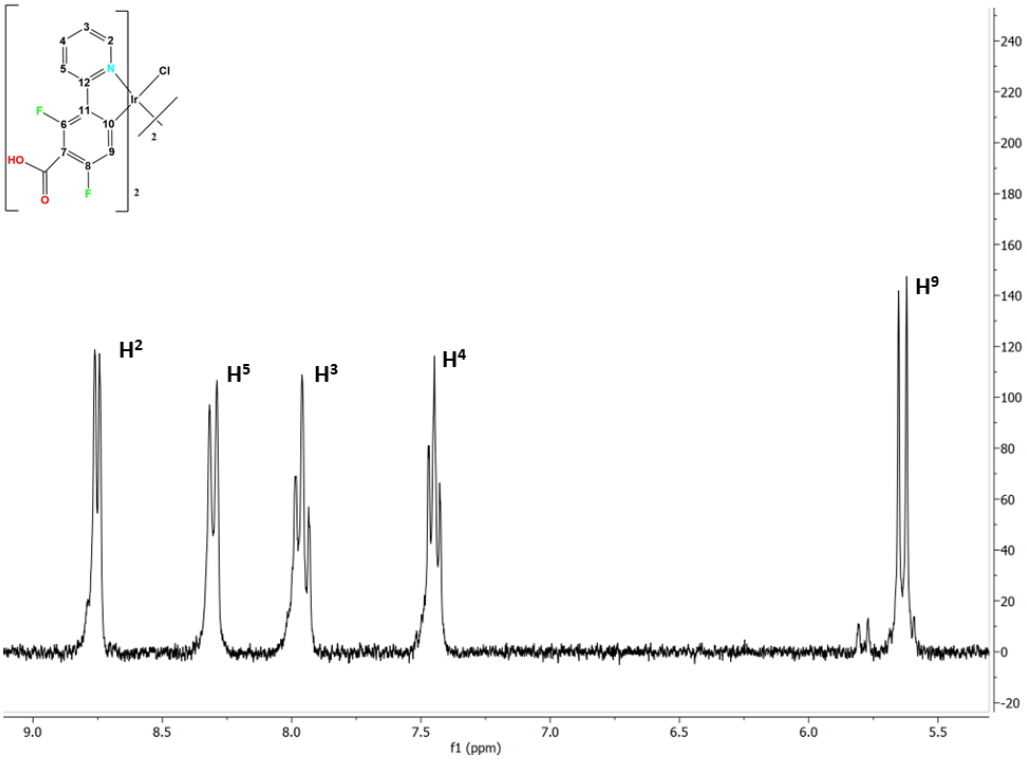

Figure S2.1. NMR ^{1}H spectra of **1c** in D_2O + KOH.

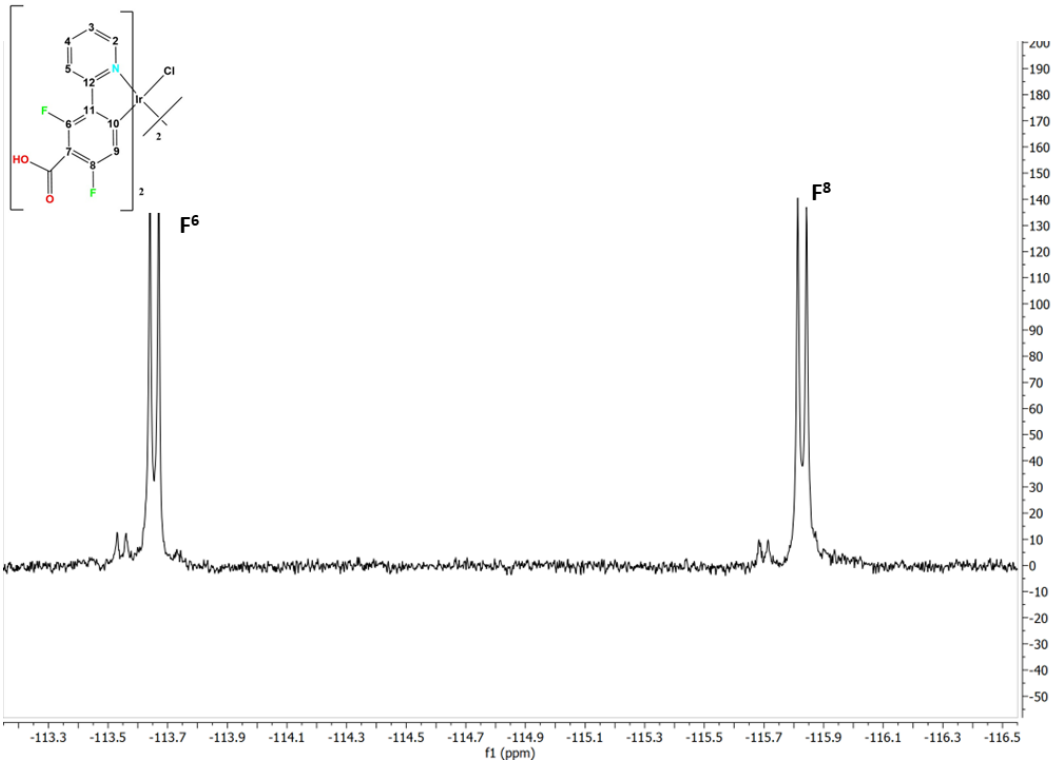

Figure S2.2. NMR ^{1}H spectra of **1c** in D_2O + KOH.

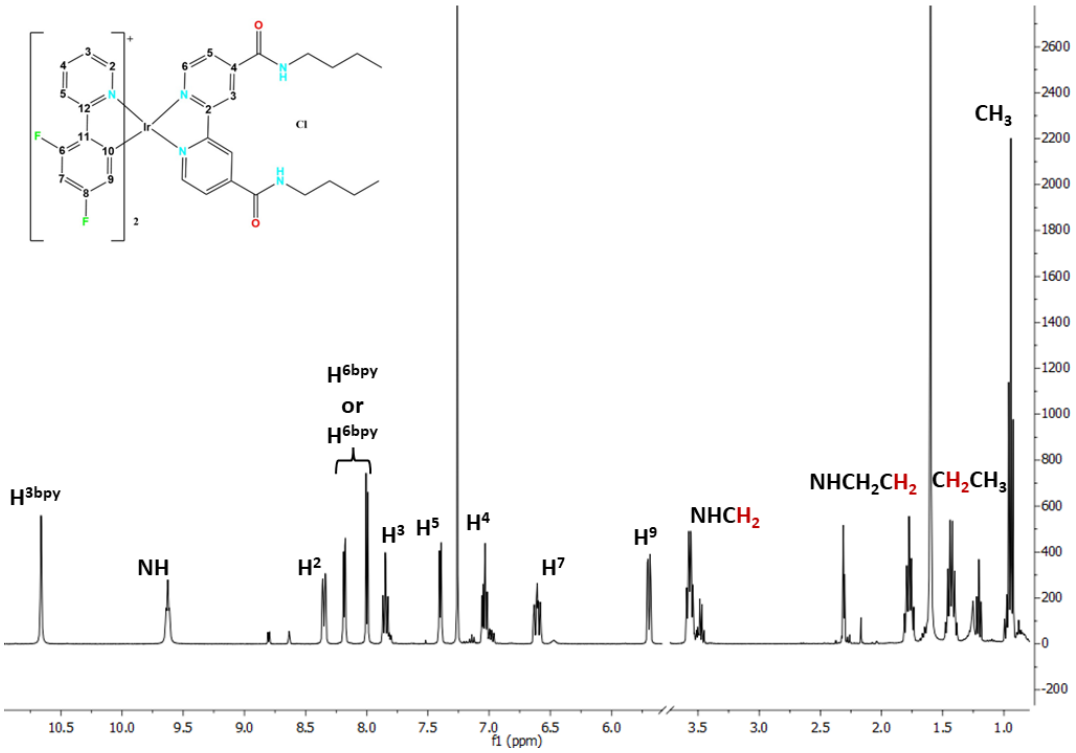

Figure S3.1. ^{1}H NMR spectra of **2a-Cl** in $CDCl_3$.

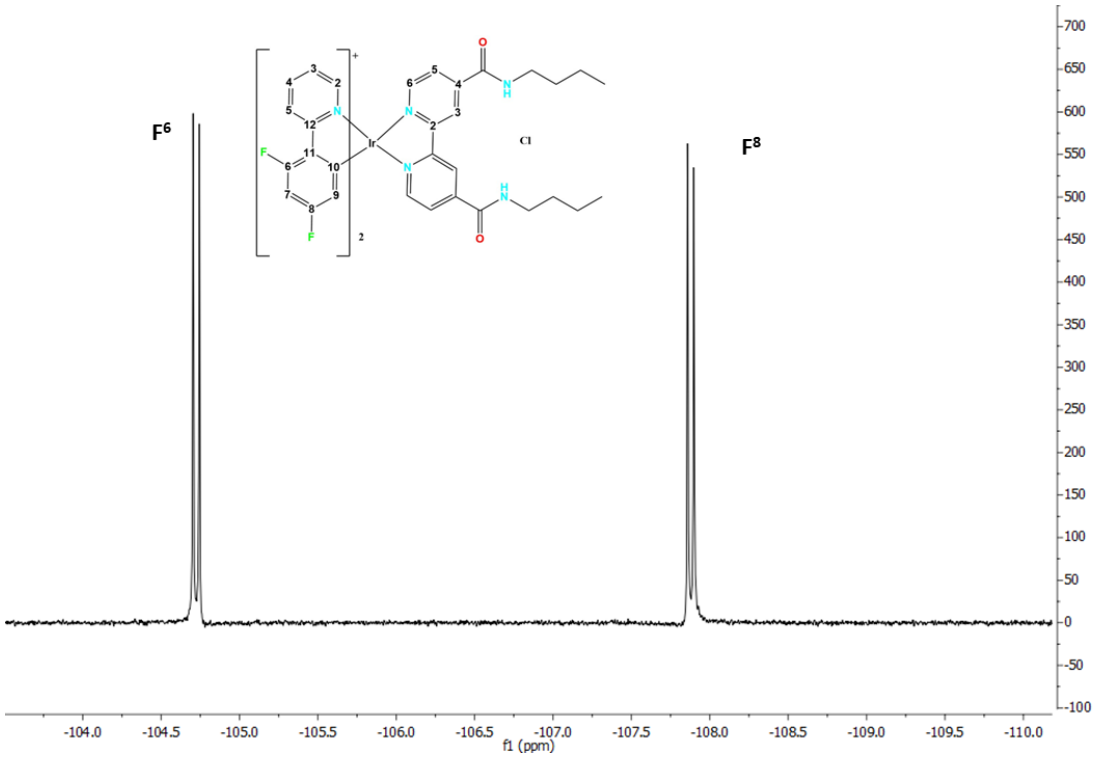

Figure S3.2. ^{19}F NMR spectra of **2a-Cl** in $CDCl_3$.

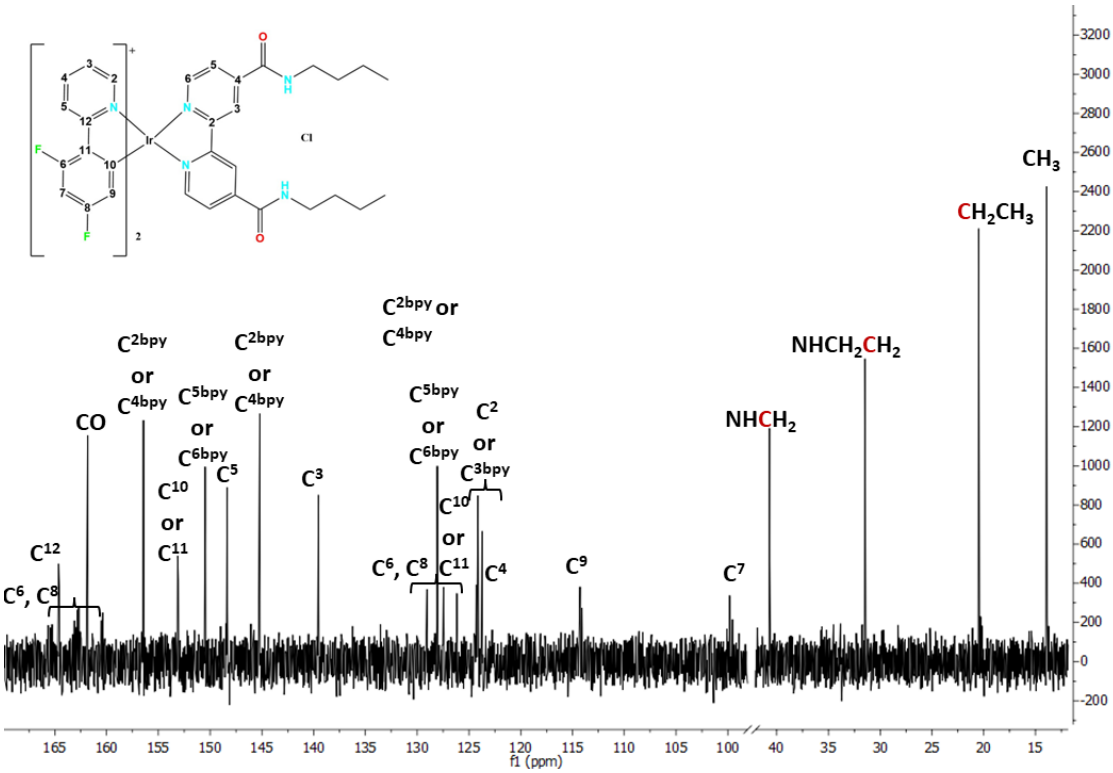

Figure S3.3. ^{13}C NMR spectra of **2a-Cl** in $CDCl_3$.

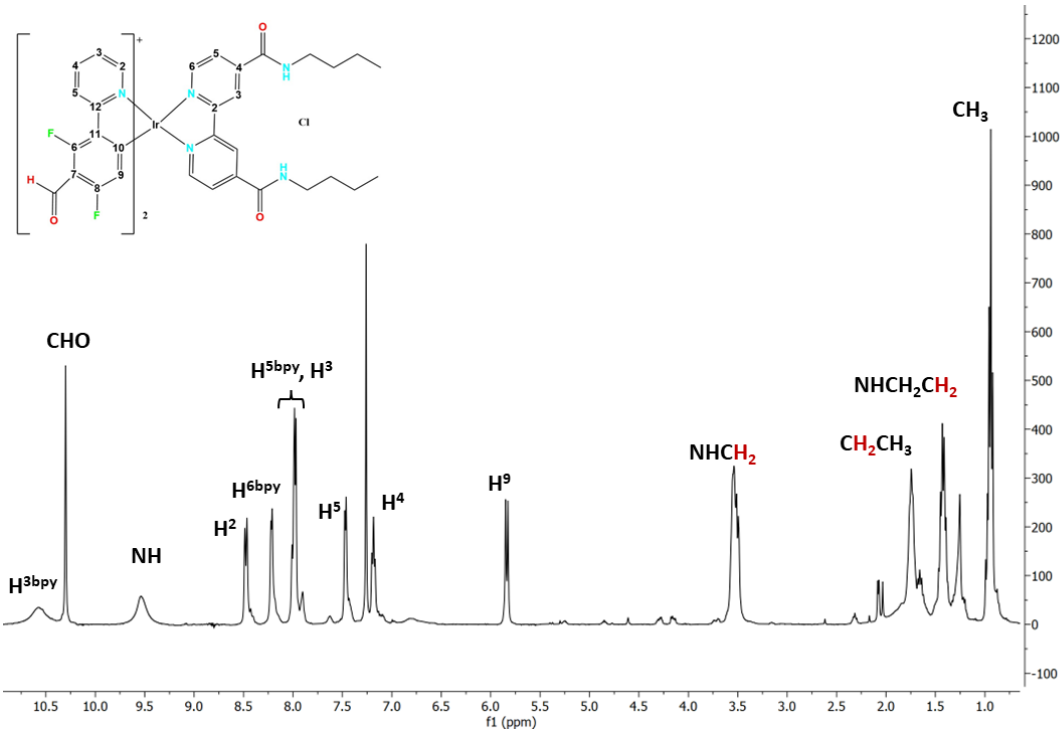

Figure S4.1. ^{1}H NMR spectra of **2b-Cl** in $CDCl_3$.

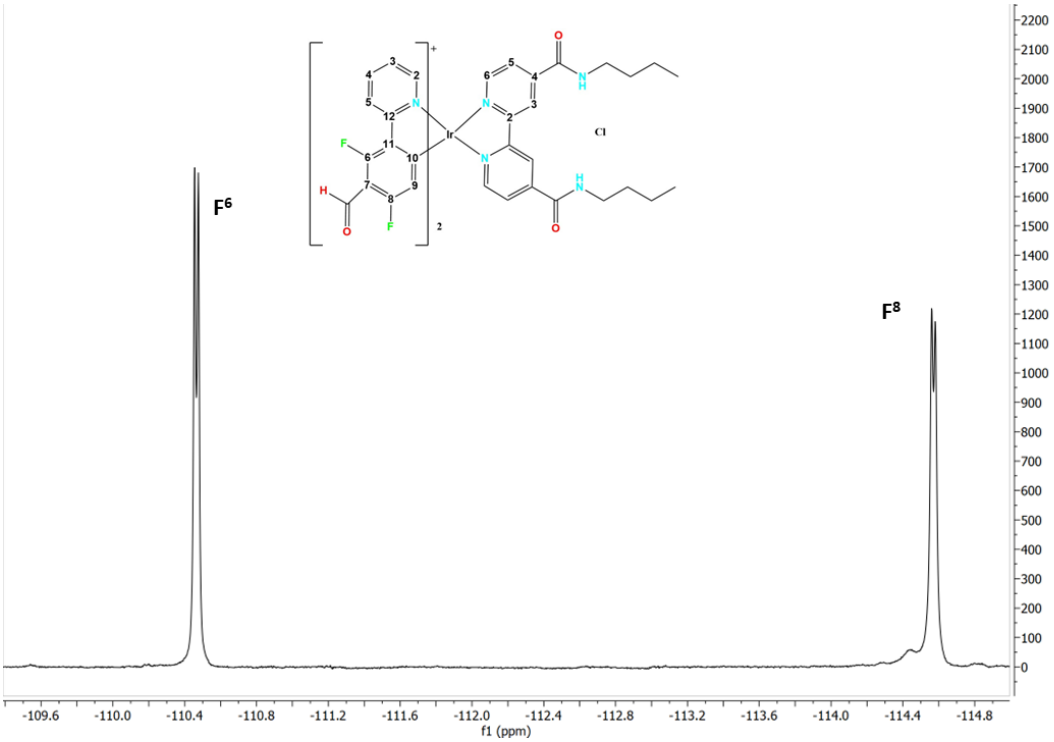

Figure S4.2. ^{19}F NMR spectra of **2b-Cl** in $CDCl_3$.

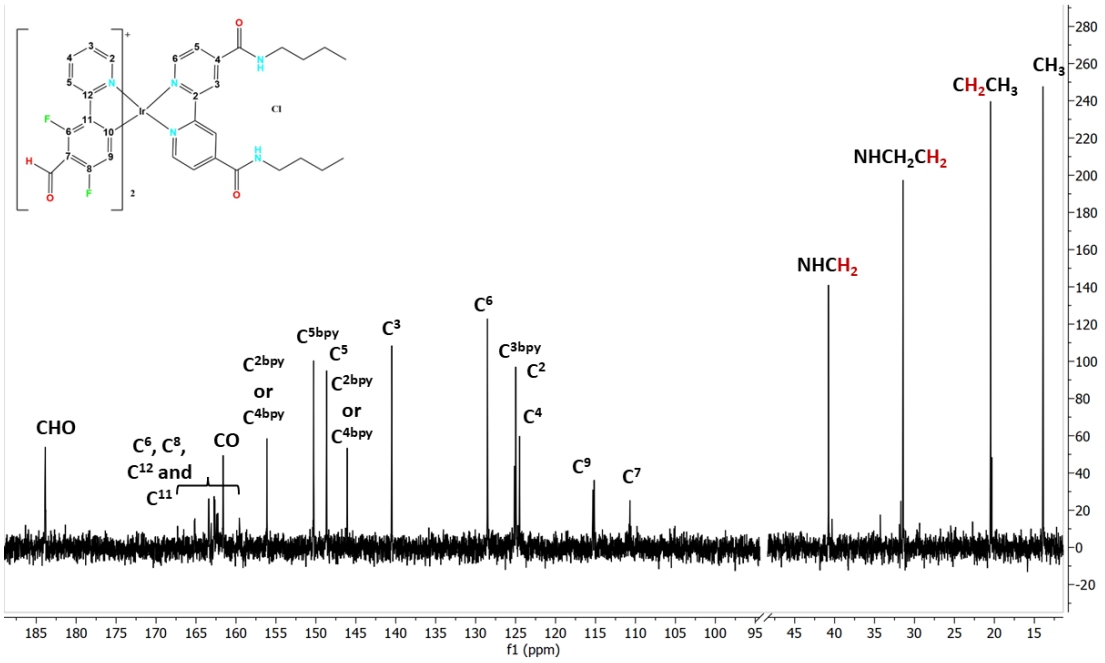

Figure S4.3. ^{13}C NMR spectra of **2b-Cl** in $CDCl_3$.

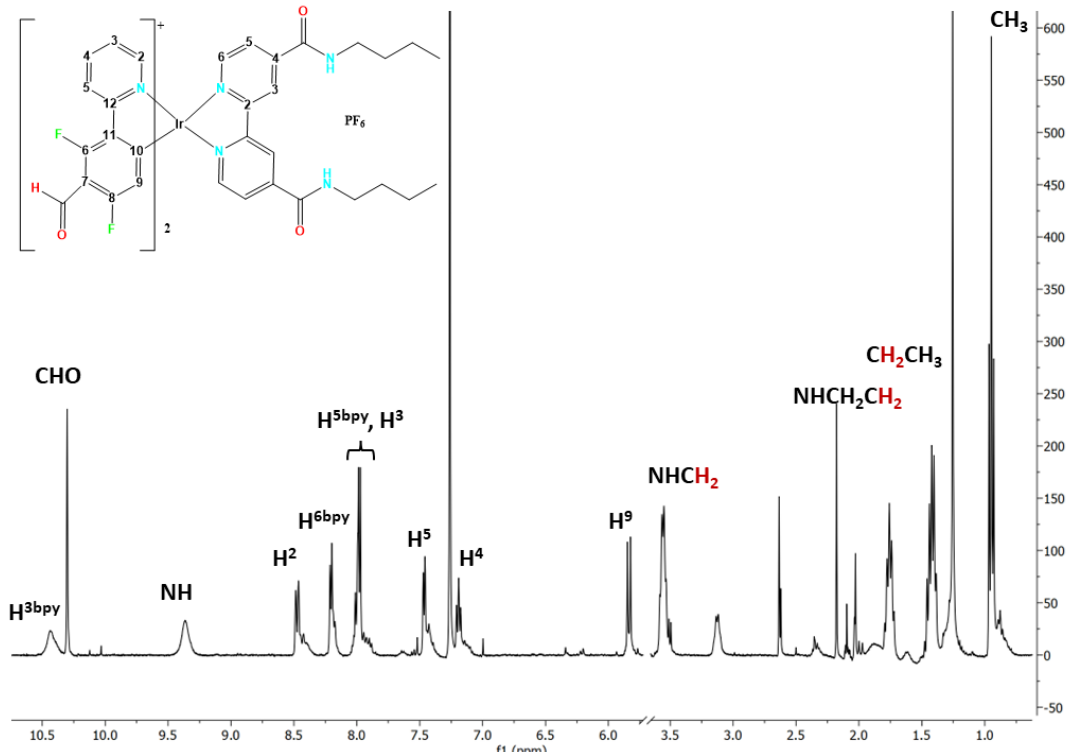

Figure S5.1. ^{1}H NMR spectra of **2b-PF_6** in $CDCl_3$.

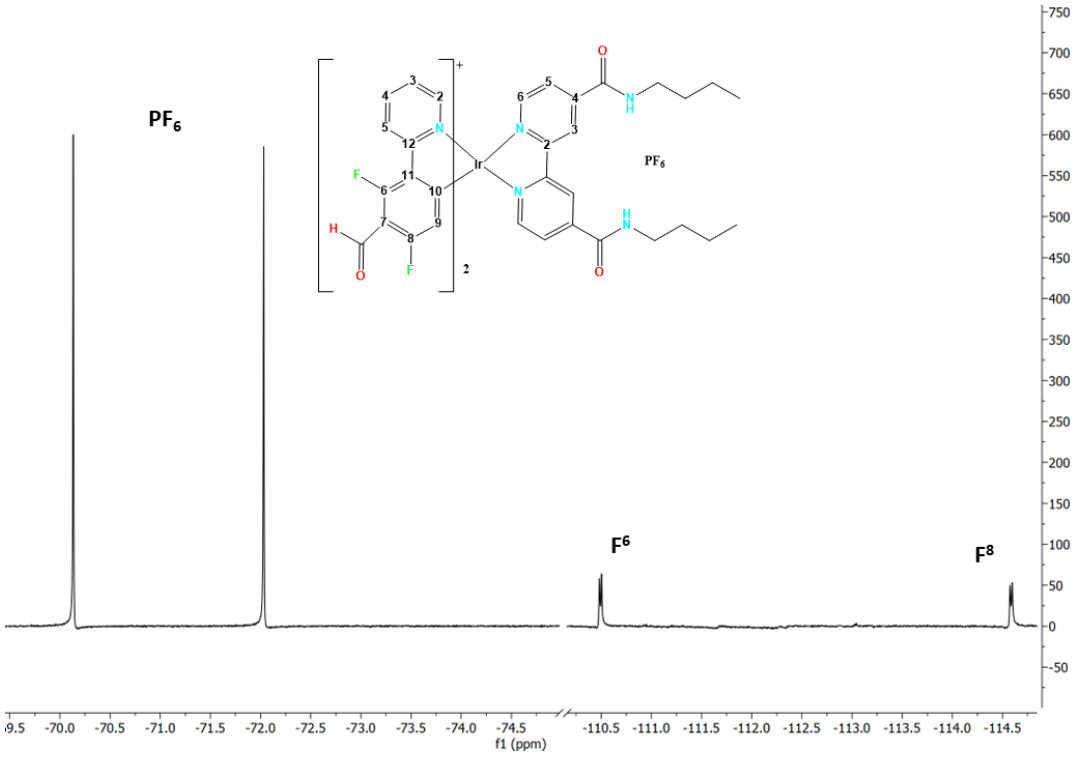

Figure S5.2. ^{19}F NMR spectra of **2b-PF$_6$** in $CDCl_3$.

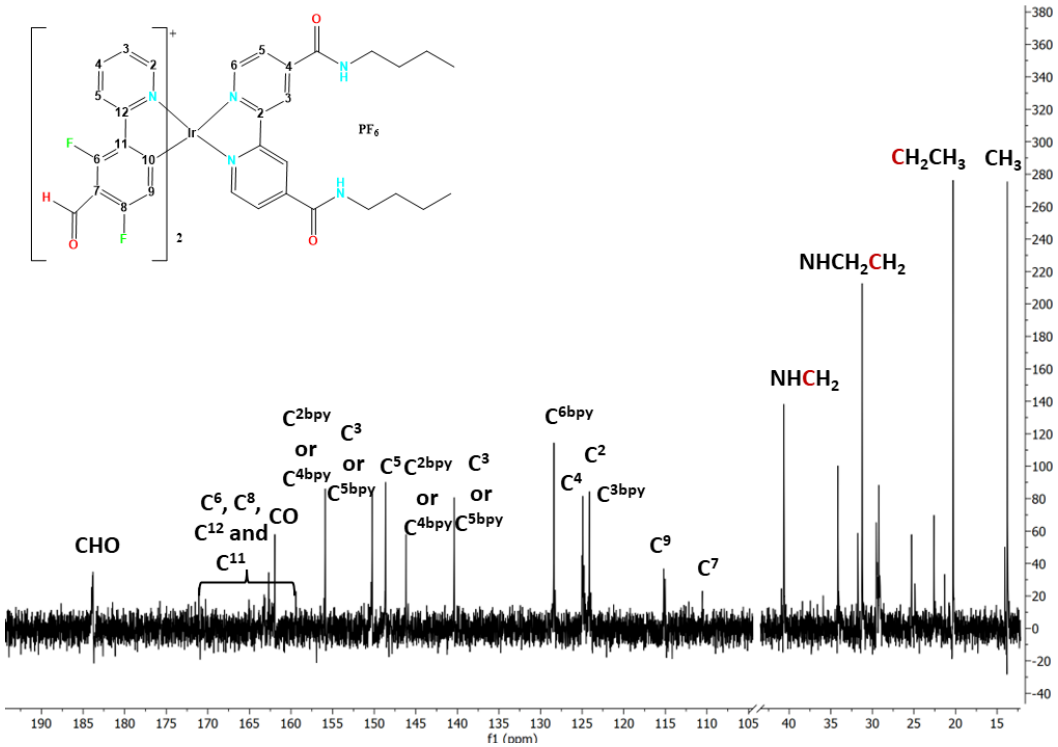

Figure S5.3. ^{13}C NMR spectra of **2b-PF$_6$** in $CDCl_3$.

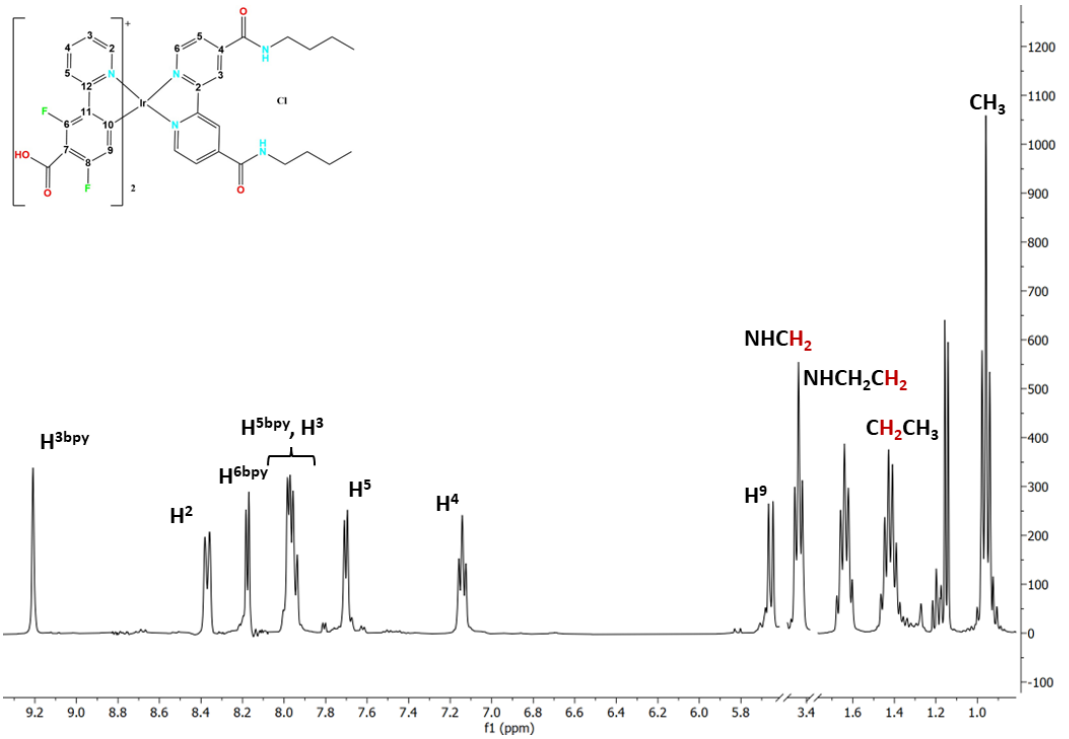

Figure S6.1. ^{1}H NMR spectra of **2c-Cl** in MeOD.

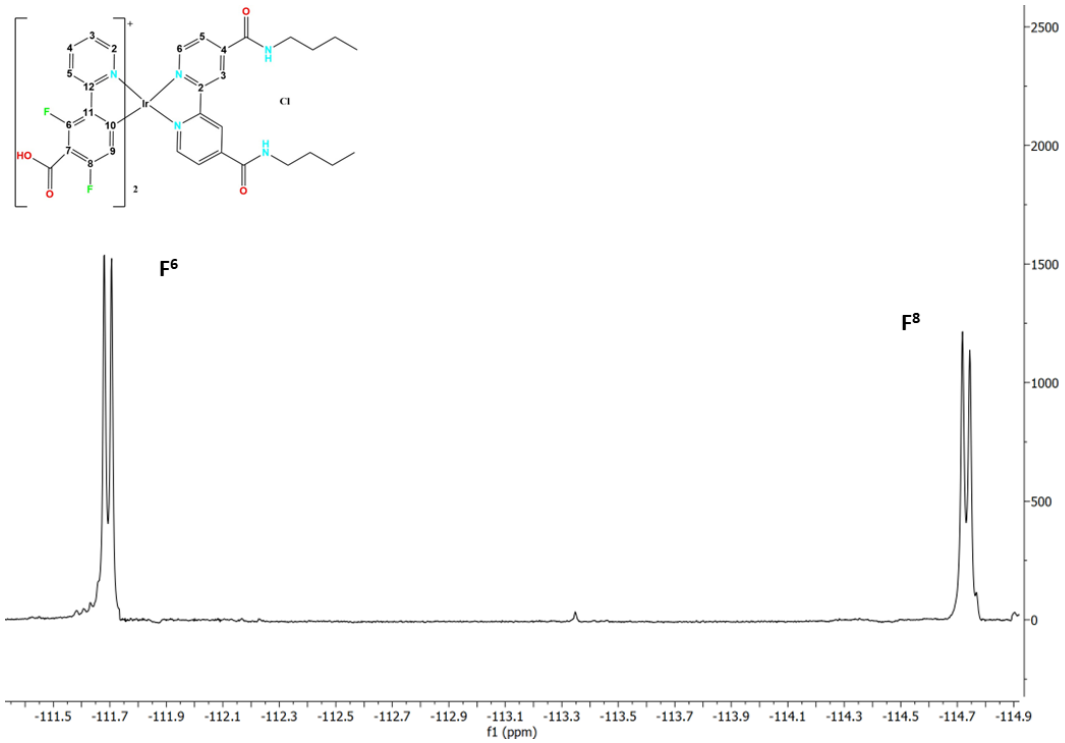

Figure S6.2. ^{19}F NMR spectra of **2c-Cl** in MeOD.

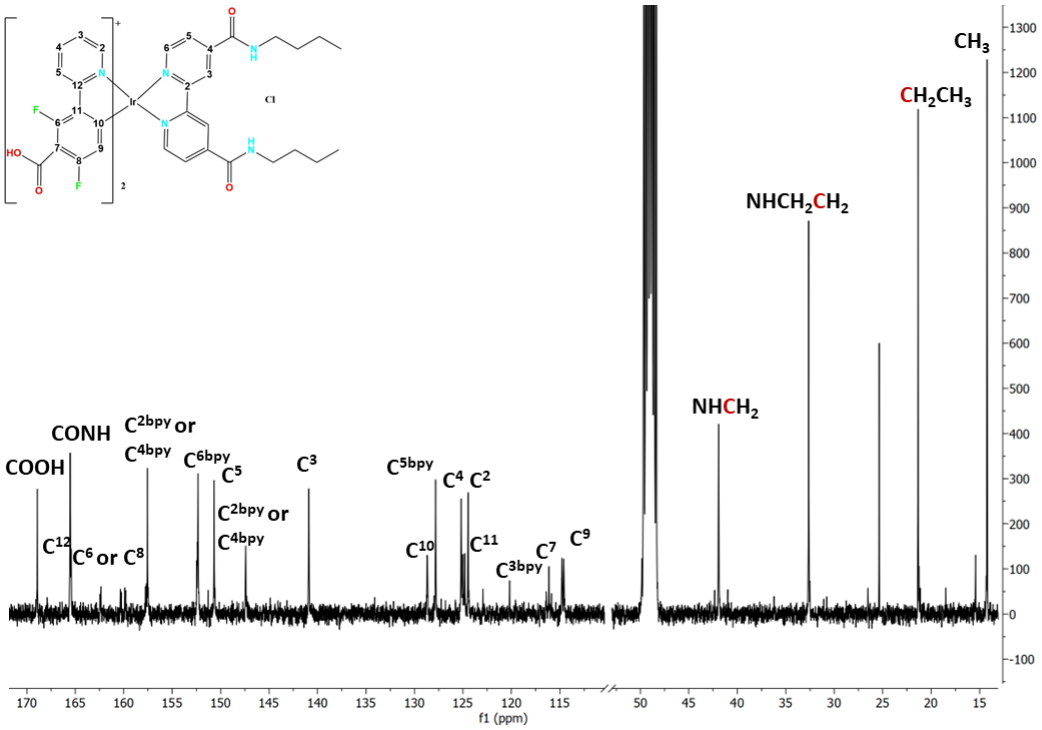

Figure S6.3. ^{13}C NMR spectra of **2c-Cl** in MeOD.

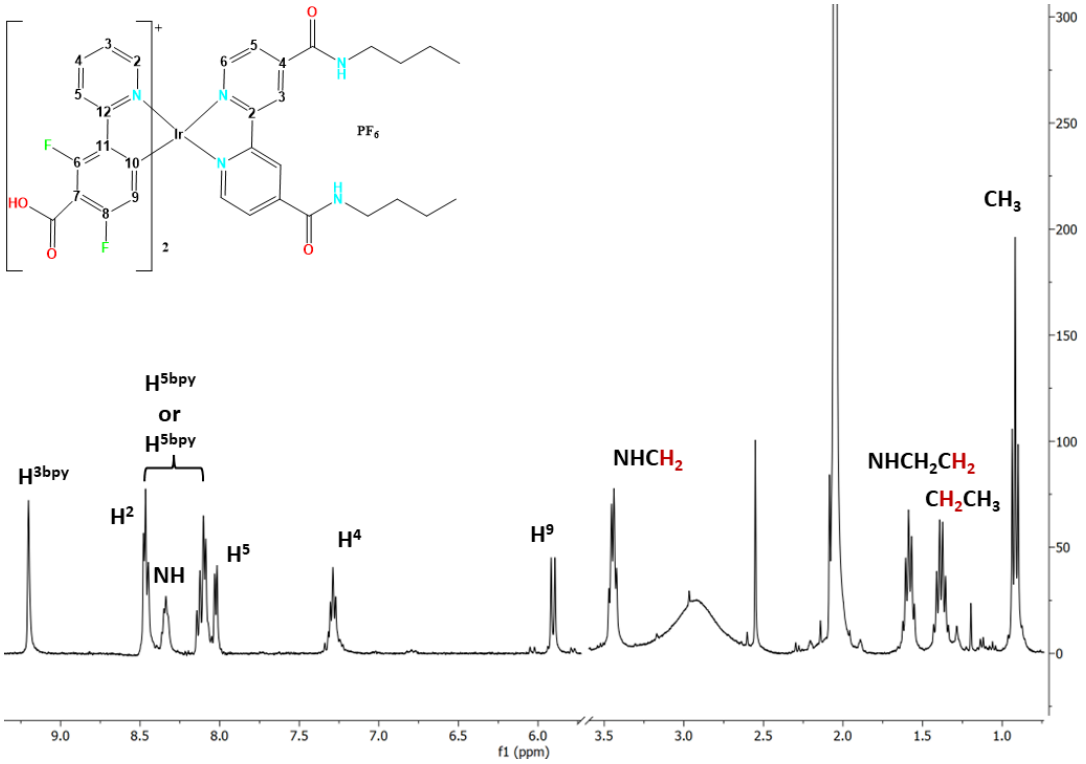

Figure S7.1. ^{1}H NMR spectra of **2c-PF$_6$** in $(CD_3)_2CO$.

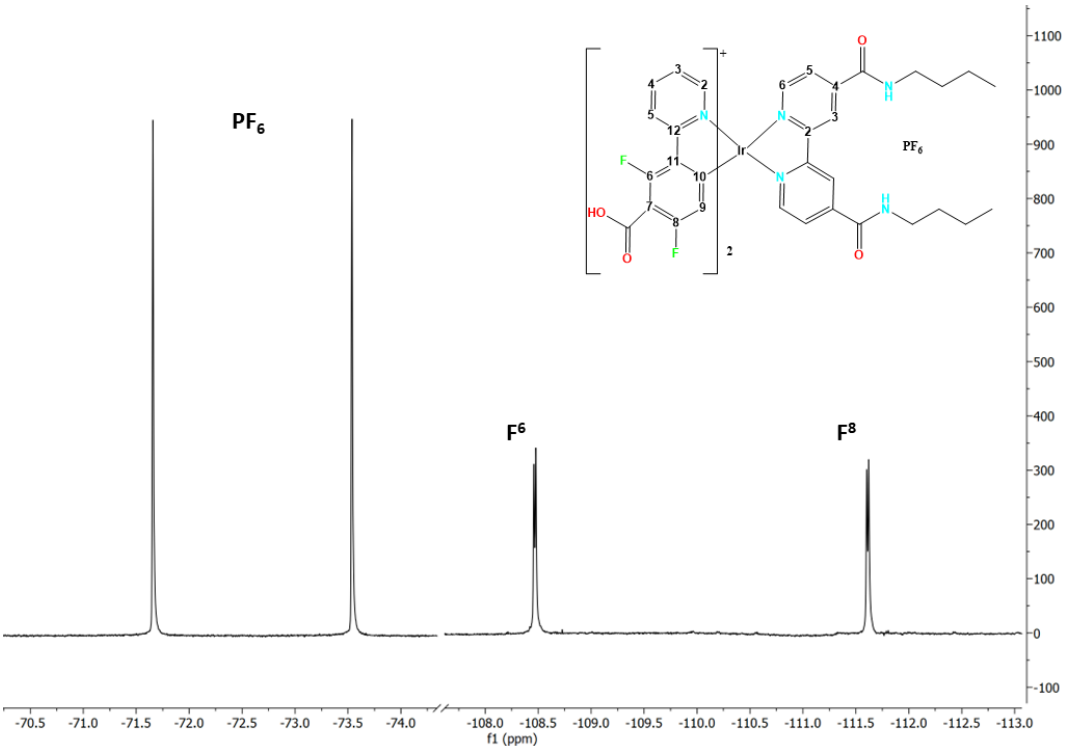

Figure S7.2. ^{19}F NMR spectra of **2c-PF$_6$** in $(CD_3)_2CO$.

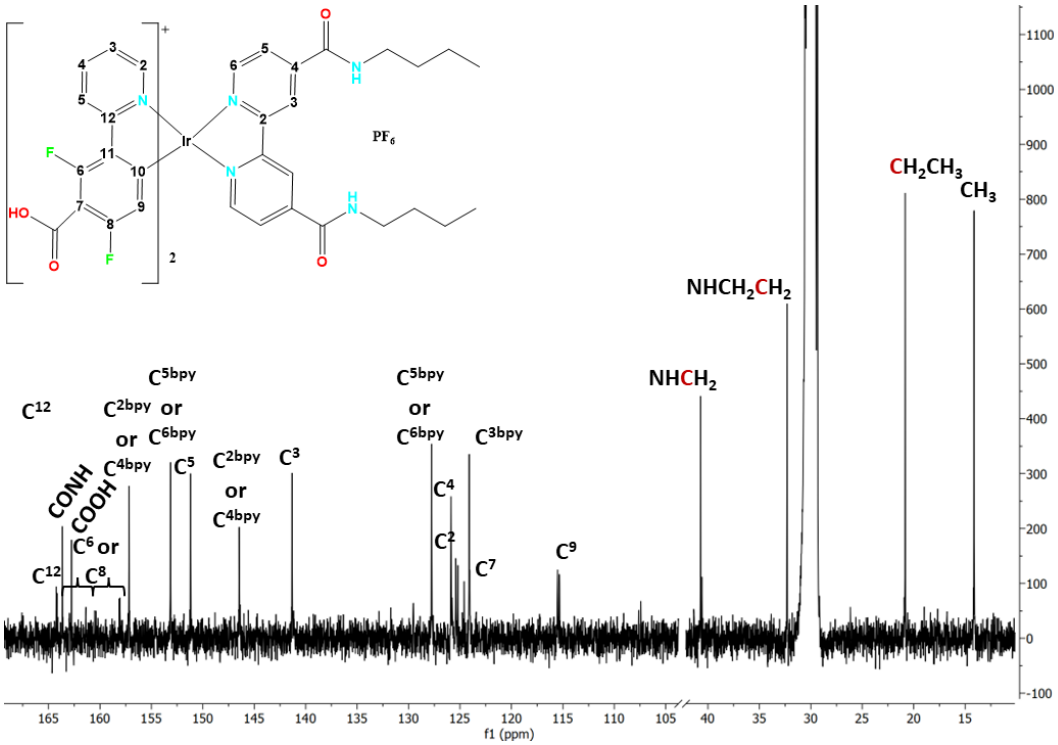

Figure S7.3. ^{13}C NMR spectra of **2c-PF$_6$** in $(CD_3)_2CO$.

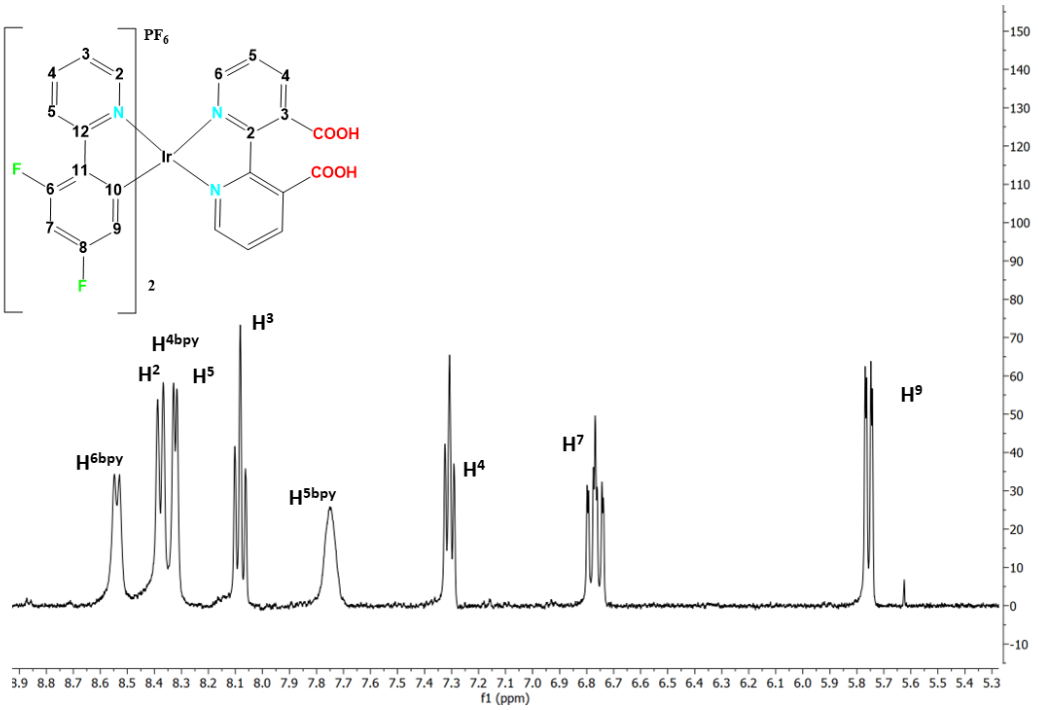

Figure S8.1. ^{1}H NMR spectra of **3a-PF$_6$** in $(CD_3)_2CO$.

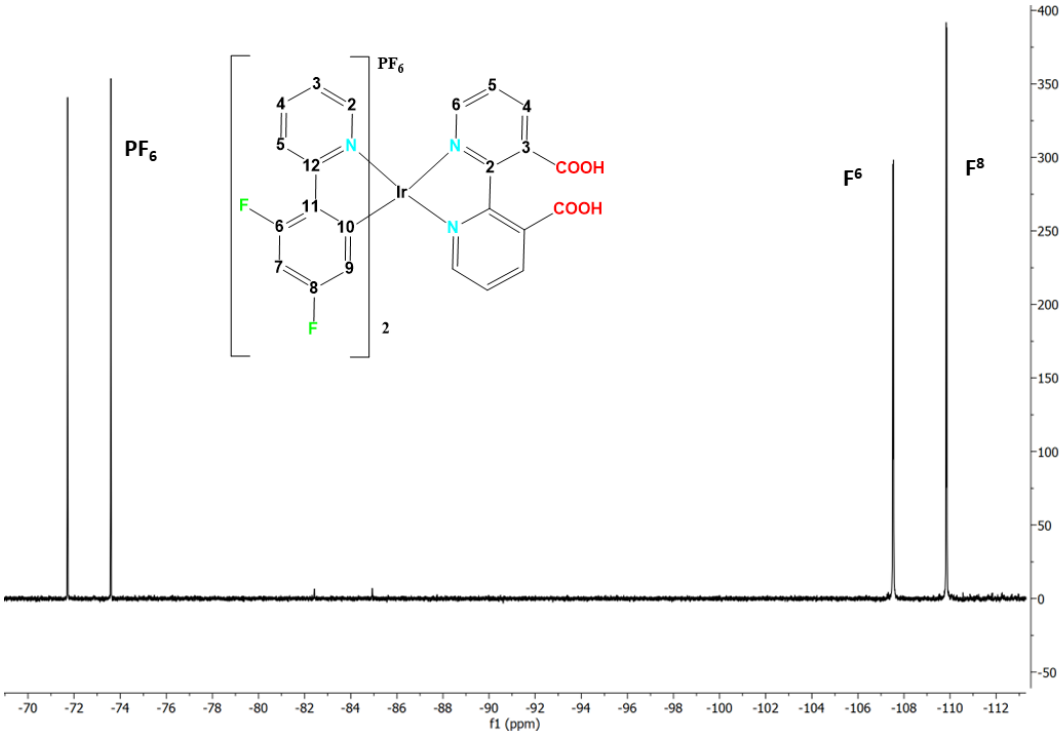

Figure S8.2. ^{19}F NMR spectra of **3a-PF$_6$** in $(CD_3)_2CO$.

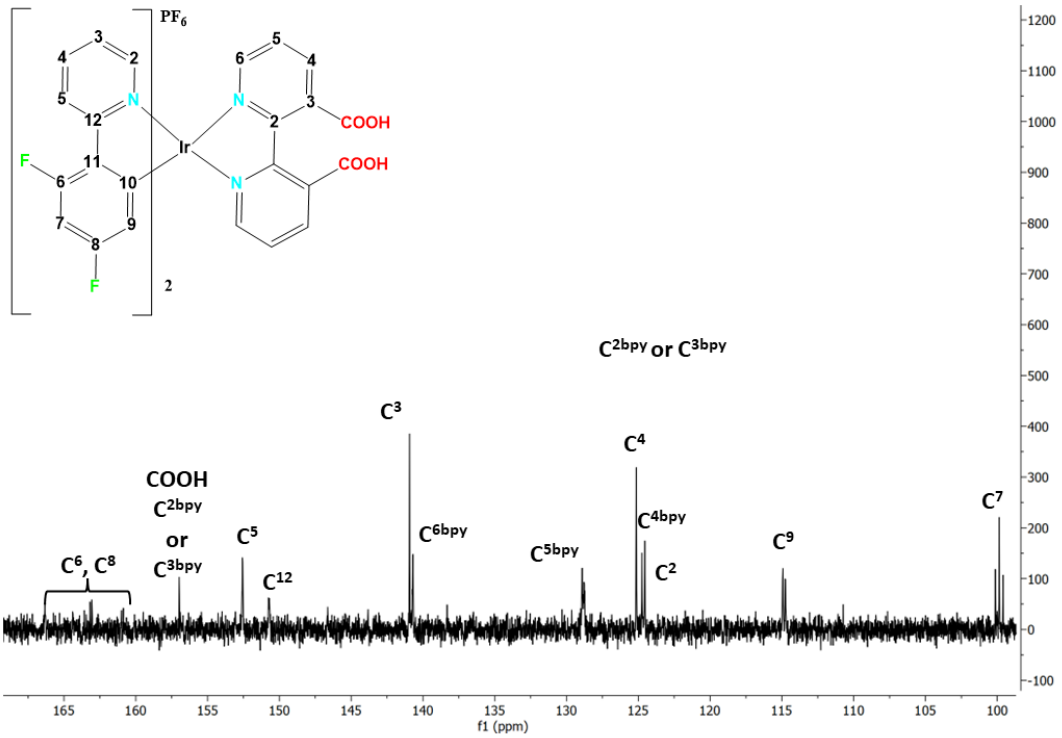

Figure S8.3. ^{13}C NMR spectra of **3a-PF$_6$** in $(CD_3)_2CO$.

3.- Crystal Structures

Selected bond lengths and angles and X-ray crystallographic data for complex **2a-Cl**·3$CHCl_3$ and **2c**-PO_2F_2·acetone are summarized in Tables S1 and S2. Yellow crystals of complex **2a** and **2c** were obtained by slow diffusion at room temperature of n-hexane or n-heptane into saturated solutions of chloroform or acetone, respectively. X-ray intensity data were collected with a Bruker D8 QUEST (PHOTON 100 CMOS) area-detector diffractometer, using graphite-monochromatic Mo-K_α radiation. The images were collected and processed using Bruker APEX3 and SAINT programs,[5] carrying out the absorption correction at this point by semi-empirical methods using SADABS.[5] The structures were solved by intrinsic phasing using SHELXT,[6] and refined by full-matrix least squares on F^2 with SHELXL,[7] using the WINGX program suite.[8] All non-hydrogen atoms were assigned anisotropic displacement parameters.

For complex **2a-Cl**, two $CHCl_3$ molecules per complex molecule were found in the electron density map. Nevertheless, further inspection of the structure with PLATON[9] and SQUEEZE[10] revealed the presence of two voids of 426 e·$Å^{-3}$ in the unit cell, each of them containing 105 electrons, which fits well for the presence of one additional molecule of $CHCl_3$ for each Iridium(III) complex molecule (**2a-Cl**·3$CHCl_3$). For **2c**-PO_2F_2·acetone, two carboxylic hydrogens (H1 and H3) were found in the electronic density map and one restrain was used to fix one of them to its corresponding oxygen atom (O1).

Finally, several restrains have been used in order to model positional disorders in the n-butylamide chains. Specifically, for **2a-Cl**·3$CHCl_3$, one aliphatic chain has been modelled (C19-C22 50/50) using two restrains, while for complex **2c**-PO_2F_2·acetone, both aliphatic chains have been modelled (C37-C40 y C42-C45 60/40) and only one restrain has been used.

Accession Codes. CCDC 2231729 and 2231730 contain the supplementary crystallographic data for this paper. These data can be obtained free of charge via www.ccdc.cam.ac.uk/data_request/cif, or by mailing data_request@ccdc.cam.ac.uk, or by contacting The Cambridge Crystallographic Data Centre, 12 Union Road, Cambridge CB2 1EZ, UK; fax: +44 1223 336033.

Table S1. Selected distances (Å) and angles (º) for $[Ir(dfppy)_2(dbbpy)]Cl\cdot 3CHCl_3$ (**2a**$\cdot 3CHCl_3$), $[Ir(COOHdfppy)_2(dbbpy)]PO_2F_2\cdot C_3H_6O$ (**2c**-$PO_2F_2\cdot C_3H_6O$).

2a-Cl$\cdot 2CHCl_3$			
Ir(1)-N(1)	2.049(2)	Ir(1)-C(10)	2.008(2)
Ir(1)-N(2)	2.125(2)	Cl(1)···H(3A)	2.458(1)
Cl(1)···H(16)	2.601(1)		
N(1)-Ir(1)-C(10)	80.46(8)	N(1)-Ir(1)-C(10')	95.73(8)
N(1)-Ir(1)-N(1′)	174.63(9)	N(2)-Ir(1)-N(2′)	73.7(1)
N(1)-Ir(1)-N(2)	96.19(7)	N(1)-Ir(1)-N(2')	88.01(7)
2c-PO_2F_2·acetone			
Ir(1)-N(1)	2.042(3)	Ir(1)-N(1′)	2.048(3)
Ir(1)-C(10)	2.009(4)	Ir(1)-C(10′)	2.002(3)
Ir(1)-N(2)	2.131(3)	Ir(1)-N(2′)	2.127(3)
C(13)-O(1)	1.316(6)	C(25)-O(3)	1.307(5)
C(13)-O(2)	1.217(6)	C(25)-O(4)	1.193(5)
N(1)-Ir(1)-C(10)	80.5(1)	N(1′)-Ir(1)-C(10′)	80.2(1)
N(1)-Ir(1)-N(1′)	174.6(1)	N(1)-Ir(1)-C(10′)	94.7(1)
N(1′)-Ir(1)-C(10)	97.3(1)	N(2)-Ir(1)-N(2′)	76.7(1)
N(2)-Ir(1)-N(1)	96.3(1)	N(2′)-Ir(1)-N(1′)	98.6(1)
N(2)-Ir(1)-N(1′)	86.3(1)	N(2′)-Ir(1)-N(1)	86.7(1)
O(1)-C(13)-O(2)	124.1(3)	O(3)-C(25)-O(4)	122.2(4)

Table S2. X-ray Crystallographic Data for $[Ir(dfppy)_2(dbbpy)]Cl\cdot 3CHCl_3$ (**2a**$\cdot 3CHCl_3$), $Ir(COOHdfppy)_2(dbbpy)]PO_2F_2\cdot$acetone (**2c**-$PO_2F_2\cdot$acetone).

Empirical formula	$C_{45}H_{41}Cl_{10}F_4IrN_6O_2$	$C_{47}H_{44}F_6IrN_6O_9P$
F_w	1320.60	1174.05
T (K)	135(1)	100(2)
Crystal system, space	Monoclinic	Monoclinic
Space Group	C2/c	P21/n
a(Å)	17.941(3)	11.1184(5)
b(Å)	28.409(5)	30.6557(17)
c(Å)	11.205(2)	13.7608(8)
α(deg)	90	90
β(deg)	110.153(6)	98.189(2)
γ(deg)	90	90
Volume (A^3)	5361.5(17)	4642.4(4)
Z	4	4
D_{calcd} (Mg/m^3)	1.636	1.680
Absorption coefficient	3.045	2.998
F(000)	2376	2344
θ range for data	2.868 to 28.281	2.867 to 27.103
No of data // restraints //	6646 // 2 // 299	10231 / 2 / 657
Goodness-of-fit on $F^{2(a)}$	1.041	1.208
Final R indexes	R_1 = 0.0235	R_1 = 0,0326
	wR_2 = 0572	wR_2 = 0.0715
R indexes (all data)[(a)]	R_1 = 0.0273	R_1 = 0,0332
	wR_2 = 0.0584	wR_2 = 0.0719
Largest diff peak and	0.947 and -0.586	1.269 and -1.530

(a) $R_1 = \Sigma(||F_o| - |F_c||)/\Sigma|F_o|$; $wR_2 = [\Sigma w(F_o^2 - F_c^2)^2/\Sigma wF_o^2]^{1/2}$; goodness of fit = $\{\Sigma[w(F_o^2 - F_c^2)^2]/(N_{obs} - N_{param})\}^{1/2}$; $w = [\sigma^2(F_o) + (g_1P)^2 + g_2P]^{-1}$; $P = [\max(F_o^2;0 + 2F_c^2]/3$.

4.- Photophysical Properties and Theoretical calculations

Calculations for complexes were carried out with the Gaussian 09 package,[11] using Becke's three-parameter functional combined with Lee-Yang-Parr's correlation functional (B3LYP) in the singlet state (S_0), and the unrestricted U-B3LYP in the triplet state (T_1).[12, 13] According to previous theoretical calculations for iridium complexes, the optimized ground state geometry were calculated at the B3LYP/LANL2DZ (Ir)/6-31G(d,p) (ligands' atoms) level. The S_0 geometry was found to be a true minimum as no negative frequencies in the vibrational frequency study of the final geometry were found. DFT and TD-DFT calculations were carried out using the polarized continuum model approach[14] implemented in the Gaussian 09 software. The MO diagrams and the orbital contributions were generated with Gaussian 09 software and Gauss-Sum[15] program, respectively. The emission energy was calculated as the difference between the optimized T_1 and the singlet state T_0. Non-covalent interactions isosurfaces were collected with Multiwfn (v 3.7).[16] These results were visualized with the Visual Molecular Dynamics (VMD) program (v 19.3)[17] for 3D plots.

Table S3a. DFT optimized geometries for ground state and triplet state of complexes complexes **2a-Cl** and **2b-Cl** in DMSO.

	2a-Cl			**2b-Cl**	
	S_0	**T_1**	**X-ray**	**S_0**	**T_1**
Ir(1)-N(1)	2.083	2.080	2.049	2.082	2.078
Ir(1)-N(1')	2.082	2.080	2.049	2.082	2.078
Ir(1)-C(10)	2.021	2.000	2.008	2.015	2.003
Ir(1)-C(10')	2.021	2.000	2.008	2.015	2.003
Ir(1)-N(2)	2.203	2.187	2.125	2.196	2.175
Ir(1)-N(2')	2.199	2.189	2.125	2.196	2.176
N(1)-Ir(1)-N(1')	173.57	176.44	174.63	174.21	176.4
N(1)-Ir(1)-C(10)	80.09	80.88	80.45	80.15	80.8
N(1')-Ir(1)-C(10')	80.06	80.85	80.45	80.15	80.79
N(1)-Ir(1)-C(10')	95.33	96.72	95.74	95.7	96.74
N(1')-Ir(1)-C(10)	95.28	96.70	95.73	95.7	96.73
N(2)-Ir(1)- N(2')	75.18	75.44	77.29	75.44	75.94
N(2)-Ir(1)-N(1)	87.92	87.14	88.01	87.79	86.53
N(2)-Ir(1)-C(10)	97.90	94.91	96.11	97.67	95.09
N(2)-Ir(1)-N(1')	97.18	95.71	96.19	96.8	96.3
N(2)-Ir(1)-C(10')	172.67	169.57	172.76	172.65	170.8
N(2')-Ir(1)-N(1)	97.32	95.81	96.19	96.8	96.28
N(2')-Ir(1)-C(10)	172.76	170.00	172.76	172.64	170.8
N(2')-Ir(1)-N(1')	87.80	87.00	88.02	87.79	86.56
N(2')-Ir(1)-C(10')	97.85	94.48	96.11	97.68	95.16

Table S3b. DFT optimized geometries for ground state and triplet state of complexes complexes **2c-Cl** and **3a-PF_6** in DMSO.

	2c-Cl			**3a-PF_6**	
	S_0	**T_1**	**X-ray**	**S_0**	**T_1**
Ir(1)-N(1)	2.055	2.078	2.042	2.078	2.083
Ir(1)-N(1')	2.055	2.078	2.048	2.013	2.080
Ir(1)-C(10)	1.999	2.002	2.009	2.079	1.997
Ir(1)-C(10')	1.999	2.001	2.002	2.011	1.997
Ir(1)-N(2)	2.158	2.18	2.131	2.219	2.195
Ir(1)-N(2')	2.158	2.18	2.127	2.223	2.080
N(1)-Ir(1)-N(1')	173.8	176.3	174.61	173.21	176.19
N(1)-Ir(1)-C(10)	80.33	80.75	80.49	80.23	80.79
N(1')-Ir(1)-C(10')	80.33	80.76	80.22	80.25	80.77
N(1)-Ir(1)-C(10')	95.24	96.73	94.68	95.35	96.57
N(1')-Ir(1)-C(10)	95.22	96.73	97.34	95.36	96.65
N(2)-Ir(1)- N(2')	76.25	75.71	76.66	74.56	74.72
N(2)-Ir(1)-N(1)	87.89	86.88	86.32	88.63	95.39
N(2)-Ir(1)-C(10)	97.48	94.76	99.12	98.69	95.56
N(2)-Ir(1)-N(1')	96.97	96.03	96.27	98.34	96.29
N(2)-Ir(1)-C(10')	173.3	170.3	173.90	172.62	170.03
N(2')-Ir(1)-N(1)	96.98	96.05	98.56	86.83	87.14
N(2')-Ir(1)-C(10)	173.3	170.2	175.70	173.90	169.80
N(2')-Ir(1)-N(1')	87.9	86.97	86.66	86.50	86.70
N(2')-Ir(1)-C(10')	97.44	94.89	97.94	98.13	95.95

Table S4. Composition (%) of Frontier MOs in the ground state for complexes **2a-Cl, 2b-Cl, 2c-Cl and 3a-PF_6** in DMSO.

2a-Cl					
MO	**eV**	**Ir**	**dfppy**	**dbbpy**	**Cl**
LUMO+5	-1.14	2	91	7	0
LUMO+4	-1.73	3	91	6	0
LUMO+3	-1.74	1	7	92	0
LUMO+2	-1.82	4	95	1	0
LUMO+1	-1.85	1	5	94	0
LUMO	-2.63	3	1	96	0
HOMO	-5.93	38	60	2	0
HOMO-1	-6.39	7	92	1	0
HOMO-2	-6.50	16	83	1	0
HOMO-3	-6.71	10	6	23	62
HOMO-4	-6.71	59	32	8	1
HOMO-5	-6.75	42	29	8	21

Table S4. Composition (%) of Frontier MOs in the ground state for complexes **2a-Cl, 2b-Cl, 2c-Cl and 3a-PF_6** in DMSO (continue)

2b-Cl					
MO	**eV**	**Ir**	**CHOdfppy**	**dbbpy**	**Cl**
LUMO+5	-1.75	0	81	18	0
LUMO+4	-1.82	1	27	72	0
LUMO+3	-1.89	1	14	85	0
LUMO+2	-1.97	6	79	15	0
LUMO+1	-2.09	5	94	2	0
LUMO	-2.71	3	1	96	0
HOMO	-6.27	36	63	2	0
HOMO-1	-6.65	7	91	2	0
HOMO-2	-6.73	0	1	19	80
HOMO-3	-6.78	19	78	2	0
HOMO-4	-6.83	0	1	6	93
HOMO-5	-6.89	0	1	21	78
2c-Cl					
MO	**eV**	**Ir**	**COOHdfppy**	**dbbpy**	**Cl**
LUMO+5	-1.21	2	93	6	0
LUMO+4	-1.71	1	10	89	0
LUMO+3	-1.74	3	66	31	0
LUMO+2	-1.81	3	29	69	0
LUMO+1	-1.87	4	95	1	0
LUMO	-2.62	3	1	96	0
HOMO	-6.49	35	63	2	0
HOMO-1	-6.88	7	91	1	0
HOMO-2	-7.00	16	82	2	0
HOMO-3	-7.12	4	3	47	46
HOMO-4	-7.17	45	28	27	0
HOMO-5	-7.21	10	5	82	3
3a-PF_6					
MO	**eV**	**Ir**	**dfppy**	**3,3´-H_2dcbpy**	-
L+5	-1.25	2	93	5	-
L+4	-1.81	4	91	5	-
L+3	-1.91	4	94	2	-
L+2	-2.11	2	4	94	-
L+1	-2.23	1	3	96	-
LUMO	-3.02	2	2	96	-
HOMO	-6.04	37	61	2	-
H-1	-6.48	6	94	1	-
H-2	-6.59	12	87	1	-
H-3	-6.86	66	29	5	-
H-4	-6.89	49	44	7	-
H-5	-6.97	18	79	3	-

Table S5. Composition (%) of frontier molecular orbitals in the first triple-state for complexes **2a-Cl, 2b-Cl, 2c-Cl and 3a-PF_6** in DMSO.

2a-Cl	**eV**	**Ir**	**dfppy**	**dbbpy**	**Cl**
SOMO	-3.53	2	1	97	0
SOMO-1	-5.12	42	55	3	0
2b-Cl	**eV**	**Ir**	**CHOdfppy**	**dbbpy**	**Cl**
SOMO	-3.65	2	1	97	0
SOMO-1	-5.48	41	51	8	0
2c-Cl	**eV**	**Ir**	**COOHdfppy**	**dbbpy**	**Cl**
SOMO	-3.60	2	1	97	0
SOMO-1	-5.37	42	53	5	0
3a-PF_6	**eV**	**Ir**	**dfppy**	**3,3´-H_2dcbpy**	-
SOMO	-4.15	2	2	96	-
SOMO-1	-5.27	40	57	3	-

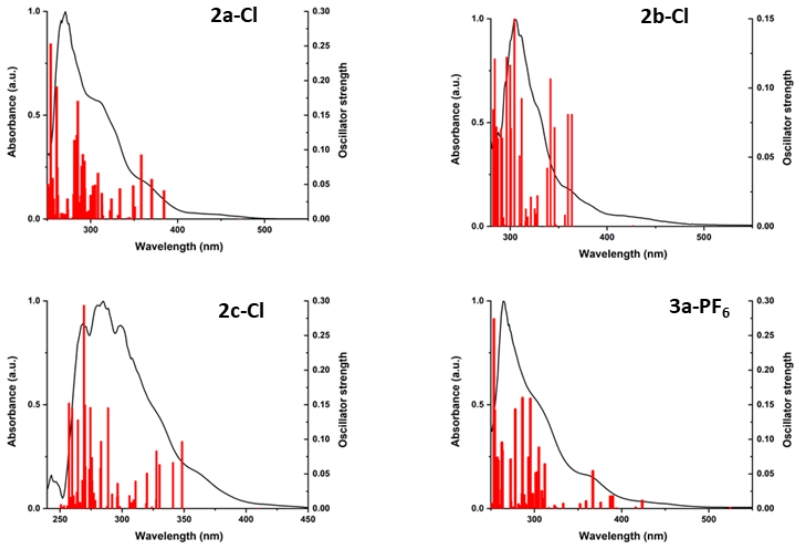

Figure S9. Calculated stick absorption spectra of **complexes 2a-Cl, 2b-Cl, 2c-Cl** and **3a-PF_6** in DMSO solution with the experimental one.

Table S6. Selected vertical excitation energies singlets (S_0) and first triplet computed in DMSO solution by TDDFT with the orbitals involved for complex **2a-Cl**, **2b-Cl**, **2c-Cl** and **3a-PF$_6$**.

	State	**λ/nm**	f	**Transition (% Contribution)**	
2a-Cl	T_1	477.98	---	HOMO→LUMO (96%)	ML'CT/LL'CT
	T_2	428.12	---	H-4→LUMO (24%), HOMO→L+2 (15%)	ML'CT/LL'CT
	T_4	423.60	---	H-1→L+2 (34%), HOMO→L+2 (35%)	ML'CT/LL'CT/IL
	S_1	471.67	0.0004	HOMO→LUMO (99%)	ML'CT/LL'CT
	S_3	384.29	0.0414	H-1→LUMO (94%)	ML'CT/LL'CT
	S_4	370.17	0.0577	HOMO→L+1 (96%)	ML'CT/LL'CT
2b-Cl	T_1	439.69	---	HOMO→LUMO (75%)	ML'CT/LL'CT
	T_2	427.76	---	H-1→L+2 (18%), HOMO→L+1 (50%)	LL'CT/IL/MLCT
	S_1	426.82	0.0007	HOMO→LUMO (98%)	ML'CT/LL'CT
	S_2	364.51	0.0004	H-8→LUMO (44%), H-3→LUMO (52%)	MLCT
	S_3	363.62	0.0811	H-1→LUMO (91%)	ML'CT/LL'CT
	S_4	359.64	0.0811	HOMO→L+1 (92%)	MLCT
	S_8	345.74	0.0717	H-7→LUMO (23%), HOMO→L+2 (56%)	MLCT/ ML'CT
	S_{10}	341.56	0.1068	H-7→LUMO (47%), HOMO→L+2 (29%)	MLCT/ ML'CT
	S_{11}	338.209	0.0422	H-6→LUMO (87%)	
2c-Cl	T_1	443.84	---	HOMO→LUMO (82%)	ML'CT/LL'CT
	T_3	416,23	---	H-1→L+3 (16%), HOMO→L+1 (41%)	ML'CT/LL'CT
	S_1	409.55	0.0007	HOMO→LUMO (97%)	ML'CT/LL'CT
	S_2	351,61	0.0008	H-5→LUMO (11%), H-4→LUMO (44%) H-2→LUMO (43%)	ML'CT/LL'CT
	S_3	348.41	0.0973	H-1→LUMO (86%)	ML'CT/LL'CT
	S_4	341.07	0.0669	HOMO→L+1 (94%)	MLCT
	S_5	330.18	0.0638	H-6→LUMO (18%), H-3→LUMO (17%), HOMO→L+2 (21%), HOMO→L+3 (30%)	L'LCT/ MLCT
	S_6	327.71	0.0837	H-6→LUMO (13%), H-3→LUMO (26%), HOMO→L+2 (27%), HOMO→L+3 (12%)	IL/ML'CT/LL'CT/ L'LCT

Table S6. Selected vertical excitation energies singlets (S_0) and first triplet computed in DMSO solution by TDDFT with the orbitals involved for complex **2a-Cl**, **2b-Cl**, **2c-Cl** and **3a-PF_6**. (continue)

	State	**λ/nm**	f	**Transition (% Contribution)**	
3a-PF_6	T_1	532.34	0.0	HOMO→LUMO (95%)	ML'CT/LL'CT
	T_2	439.04	0.0	H-6→LUMO (26%), H-3→LUMO (43%), H-2→LUMO (15%)	ML'CT/LL'CT
	T_3	437.79	0.0	H-4→LUMO (22%), H-1→LUMO (57%)	ML'CT/LL'CT
	S_1	524.60	0.0008	HOMO→LUMO (98%)	ML'CT/LL'CT
	S_2	423.61	0.0114	H-1→LUMO (94%)	LL'CT
	S_5	389.88	0.0178	H-4→LUMO (66%), HOMO→L+1 (18%)	ML'CT/LL'CT
	S_6	386.89	0.0174	H-4→LUMO (16%), HOMO→L+1 (73%)	ML'CT/LL'CT
	S_8	367.00	0.0541	HOMO→L+3 (93%)	MLCT
	S_9	359.24	0.0104	H-5→LUMO (86%), H-4→LUMO (12%)	ML'CT/LL'CT
	S_{15}	311.86	0.0638	H-4→L+1 (22%), H-1→L+3 (42%)	ML'CT/LL'CT
	S_{16}	311.11	0.0143	H-4→L+1 (24%), H-1→L+3 (36%)	ML'CT/LL'CT
	S_{18}	308.45	0.0252	H-4→L+1 (13%), H-3→L+3 (21%), H-2→L+3 (45%)	ML'CT/LL'CT
	S_{19}	305.00	0.088	H-2→L+3 (10%), H-1→L+4 (62%), HOMO→L+5 (15%)	MLCT
	S_{20}	303.55	0.0524	H-3→L+2 (52%), H-2→L+2 (18%)	MLCT
	S_{21}	301.85	0.0232	H-4→L+2 (10%), HOMO→L+5 (57%)	MLCT
	S_{22}	301.55	0.0515	H-4→L+2 (40%), H-3→L+4 (10%), H-2→L+4 (12%), HOMO→L+5 (10%) H-9→LUMO (10%), H-6→LUMO (45%), H-4→L+2 (11%), H-3→L+2	MLCT
	S_{25}	295.25	0.1587	(10%)	MLCT
	S_{26}	293.22	0.0737	H-3→L+3 (42%), H-2→L+3 (25%)	MLCT
	S_{31}	286.29	0.1598	H-4→L+4 (56%)	MLCT

Table S7. Absorption data in solution ($5x10^{-5}$ M) of complexes **1-3**.

Complex	Medium	λ_{abs}/ nm (ε/ x 10^{-3}/ M^{-1} cm^{-1})
1b	**DMSO**	293 (29.96), 333 (9.72), 366 (5.58)
1c	**DMSO**	277 (60.2), 292 (52.4), 365 (9.6)
2a-Cl	**DMSO**	273 (62.6), 310 (33.8), 368 (9.5), 447 (1.3), 469 (0.7)
	THF	262 (67.9), 306 (29.9), 365 (9.9), 444 (1.3), 467 (0.8)
	Toluene	287 (56.9), 308 (47.8), 363 (12.3), 432 (2.8), 463 (1.6)
		328 (13.7), 358 (4.4), 421 (1.1)
2b-Cl	**DMSO**	306 (23.8), 328 (13.7), 358 (4.4), 421 (1.1)
	THF	293 (40.0), 300 (37.6), 331_h (17.6), 359_h (7.2), 429 (0.8)
	Toluene	287 (14.3), 336_h (3.9), 361(1.8), 387 (0.7),
2b-PF_6	**DMSO**	276 (43.2), 305 (32.5), 332 (19.4), 358 (7.8), 421 (1.0)
2c-Cl	**DMSO**	269 (54.2), 284 (60.4), 300 (52.4), 365 (9.6), 409 (1.4)
	THF	240 (51.3), 258 (57.2), 305 (24.3), 333 (14.2), 364 (5.2)
	H_2O	249 (22.2), 270 (17.2), 311 (8.6), 358 (3.0)
2c-PF_6	**DMSO**	281 (51.4), 300 (34.2), 363 (8.6), 431 (2.4)
3a-PF_6	**DMSO**	265(41.8), 305_h (20.94), 361 (6.48), 435 (0.93)

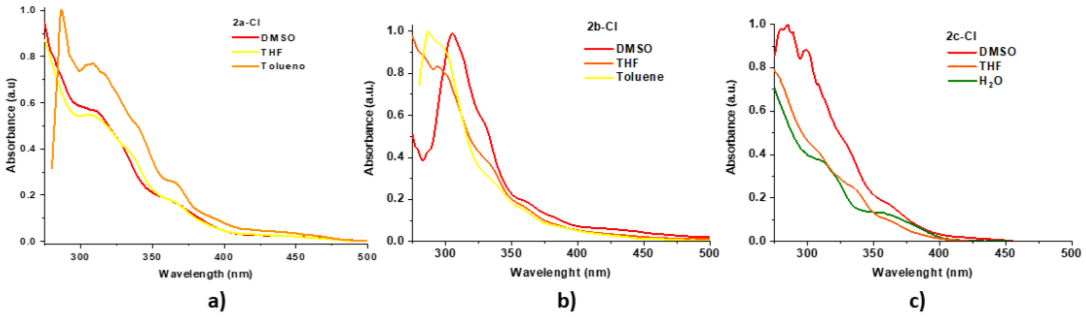

Figure S.10. Normalized absorption spectra of all complexes **2-Cl** in different solvents ($5x10^{-5}$ M).

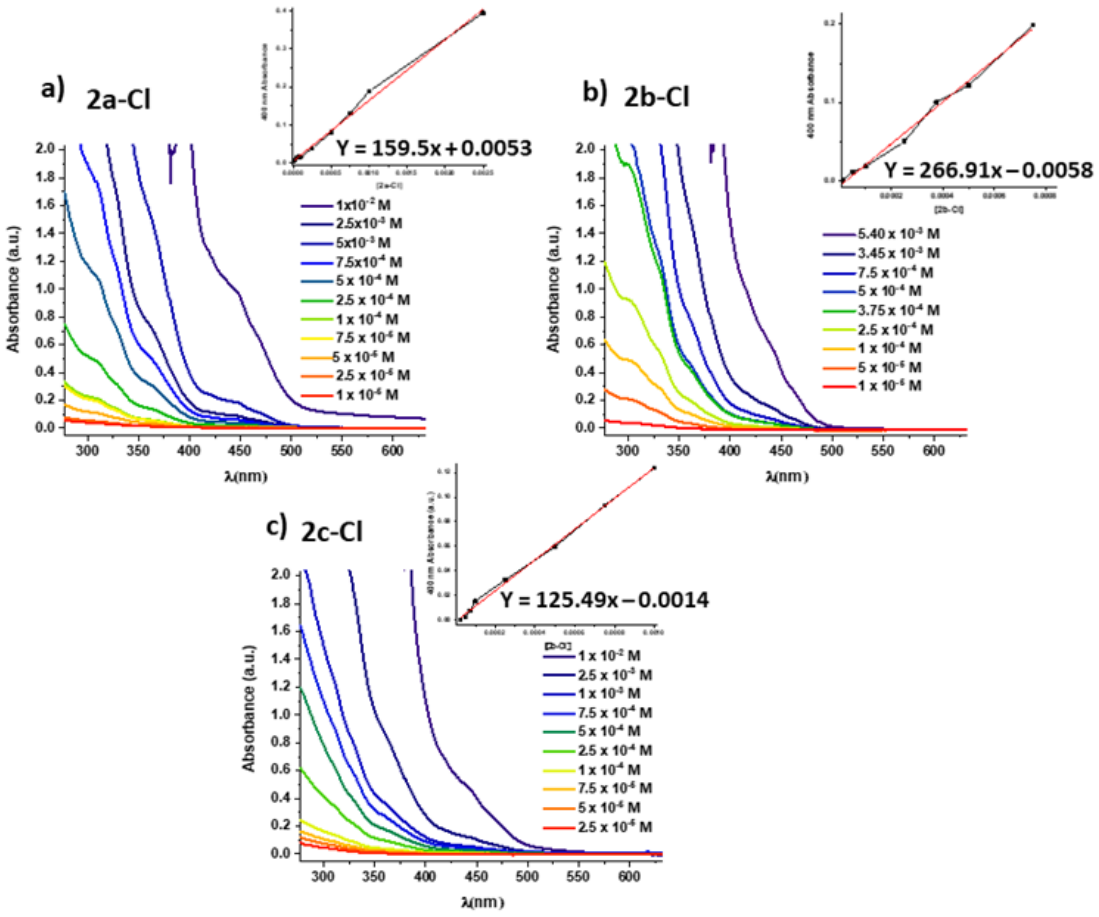

Figure S11. Low-energy region of the UV–vis absorption spectra of a) **2a-Cl**, b) **2b-Cl** and c) **2c-Cl** in DMSO at different concentrations ($1 \cdot 10^{-6}$ to $1 \cdot 10^{-2}$ M). Inset: Lineal fit of the absorbance at the 400 nm band versus concentration.

Table S8. Experimental emission data in solid state and deoxygenated solution ($5x10^{-4}$ M). Radiative (K_r) and non-radiative (K_{nr}) constants calculated at room temperature.

Complex	Medium	λ_{em}/ nm[a]	τ/μs	φ	K_r	K_{nr}
1c	Solid	540_h, 580	11.84 (40%), 1.00 (60%) [b]	0.005	$9.8\cdot10^2$	$1.9\cdot10^5$
	DMSO	510	10.14	0.02	$1.5\cdot10^3$	$9.7\cdot10^4$
2a-Cl	Solid	533	0.24 (45%), 0.59 (55%) [b]	0.42	$9.6\cdot10^5$	$1.3\cdot10^6$
	Toluene	495	1.21 (14%), 0.84 (86%) [b]	0.74	$8.2\cdot10^5$	$2.9\cdot10^5$
	THF	520	0.92 (91%), 0.14 (9%) [b]	0.70	$8.1\cdot10^5$	$3.6\cdot10^5$
	DMSO	568	0.81	0.53	$6.6\cdot10^5$	$5.7\cdot10^5$
2b-Cl	Solid	540_h, 582	0.32	0.00	$1.3\cdot10^4$	$3.1\cdot10^6$
	Toluene	503	0.64	0.23	$3.6\cdot10^5$	$1.2\cdot10^6$
	THF	507	0.70	0.28	$4.0\cdot10^5$	$1.0\cdot10^6$
	DMSO	540	0.72	0.51	$7.1\cdot10^5$	$6.8\cdot10^5$
2b-PF_6	Solid	510, 585_h	0.40	0.03	$7.8\cdot10^4$	$2.4\cdot10^6$
	DMSO	542	0.58	0.45	$7.7\cdot10^5$	$9.6\cdot10^5$
2c-Cl	Solid	530	0.47	0.21	$4.4\cdot10^5$	$1.7\cdot10^6$
	H_2O	615	0.06	0.03	$5.6\cdot10^5$	$1.7\cdot10^7$
	THF	517	0.81	0.15	$1.8\cdot10^5$	$1.0\cdot10^6$
	DMSO	558	0.76	0.54	$7.1\cdot10^5$	$6.1\cdot10^5$
2c-PF_6	Solid	595	0.62	0.03	$5.5\cdot10^4$	$1.6\cdot10^6$
	DMSO	558	0.73	0.54	$7.4\cdot10^5$	$6.3\cdot10^5$
3a-PF_6	Solid	595	0.58	0.03	$5.7\cdot10^4$	$1.7\cdot10^6$
	DMSO	605	0.31	0.04	$1.4\cdot10^5$	$3.1\cdot10^6$

a) Data measured by excitation in the range 365–400 nm. b) Emissions lifetimes with a bi-exponential decay.

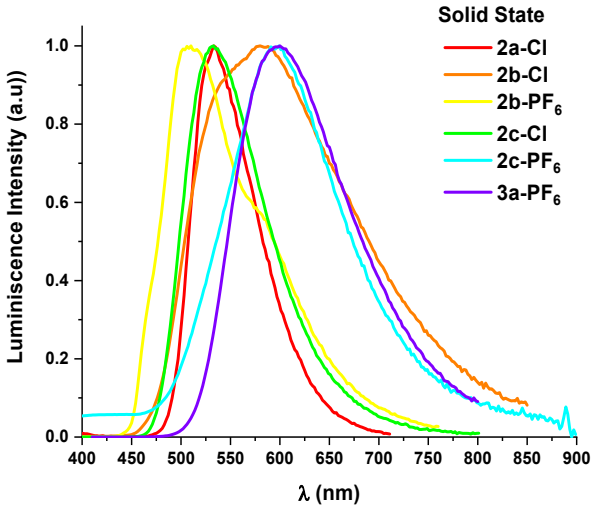

Figure S12. Emission spectra of all complexes in solid state.

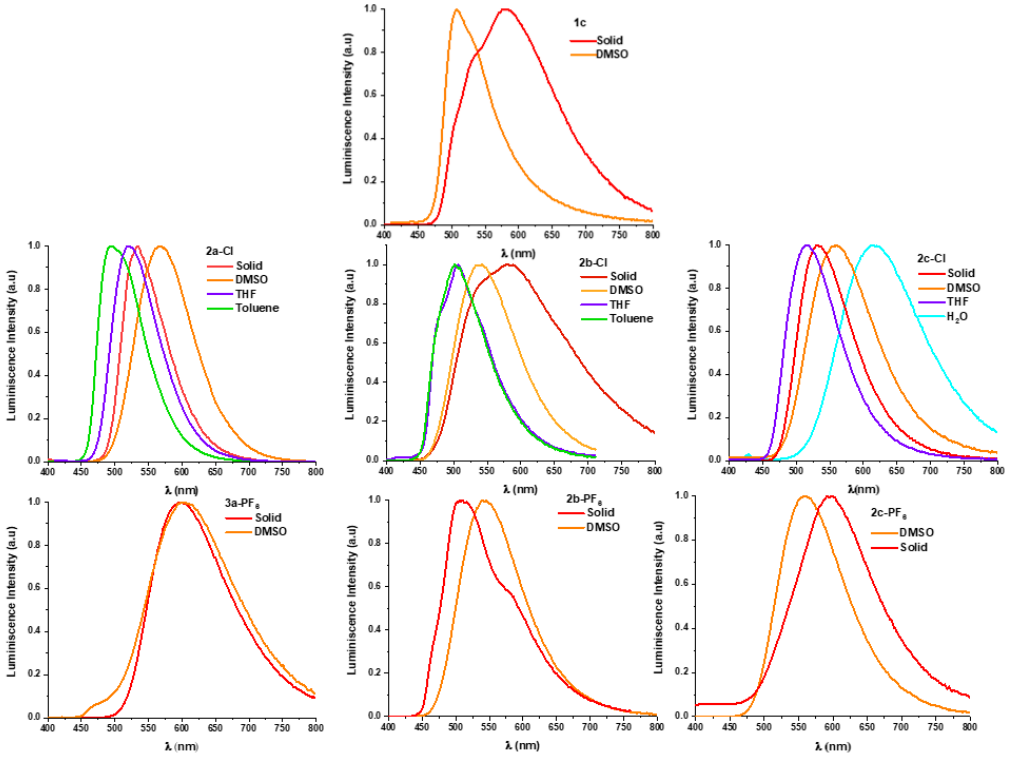

Figure S13. Emission spectra of all complexes in different solvents ($5x10^{-4}$ M).

Determination of $^1O_2$ generation quantum yields. Singlet Oxygen quantum yields (φ_Δ^{PC}) were determined according to a relative procedure adapted from the literature,[18-20] which is based on monitoring by UV-Vis spectroscopy the oxidation of 1,3-diphenylisobenzofuran (DPBF, yellow) to 1,2-dibenzoylbenzene (colorless) photosensitized by $[Ru(bpy)_3]Cl_2$ in acetonitrile solution.

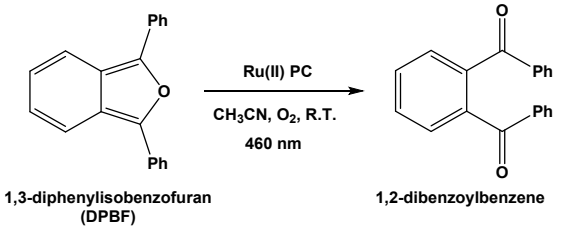

DPBF was selected as the $^1O_2$ scavenger due to its fast reaction with $^1O_2$. Air-equilibrated acetonitrile solutions containing DPBF were prepared (~8 x 10^{-5} M) in a cuvette and their absorbance adjusted to around 1.0 at 410 nm. Then, the photosensitizer ($[Ru(bpy)_3]Cl_2$, 10^{-5} M, corresponding to absorbance around 0.2) was introduced in the cuvette.

Low dye concentrations were used to minimize quenching of $^1O_2$ by the dyes. The mixture was irradiated with a blue LED strip (λ_{irr} = 460 nm) at room temperature for 0.5 seconds irradiation intervals during a total exposure period of 180 seconds and absorption UV-Vis spectra were recorded after every irradiation interval.

The decrease in the absorption band at 410 nm was plotted *vs.* the irradiation time and the experimental data were fitted to a straight line.

An acetonitrile solution of DPBF without the Ru(II) complex was examined to confirm its photostability under identical irradiation conditions (20 s). The φ_Δ^{PC} were calculated by a relative method using equation (1), and $[Ru(bpy)_3]Cl_2$ as the reference for $^1O_2$ photosensitization in acetonitrile (φ_Δ^{S} = 0.56).[21]

$$\varphi_\Delta^{PC} = \varphi_\Delta^{S} \times (S^{PC} \times F^{S}) / (S^{S} \times F^{PC}) \qquad \text{eq (1)}$$

Where S, is the slope of a linear fit for the change in absorbance of DPBF (at 410 nm) with the irradiation time, and F, is the absorption correction factor, which is given by F = 1×10^{-OD} (where OD is the optical density at the irradiation wavelength). The superscripts PC and S stand for the Ru(II) photocatalysts and the standard sensitizer, respectively.

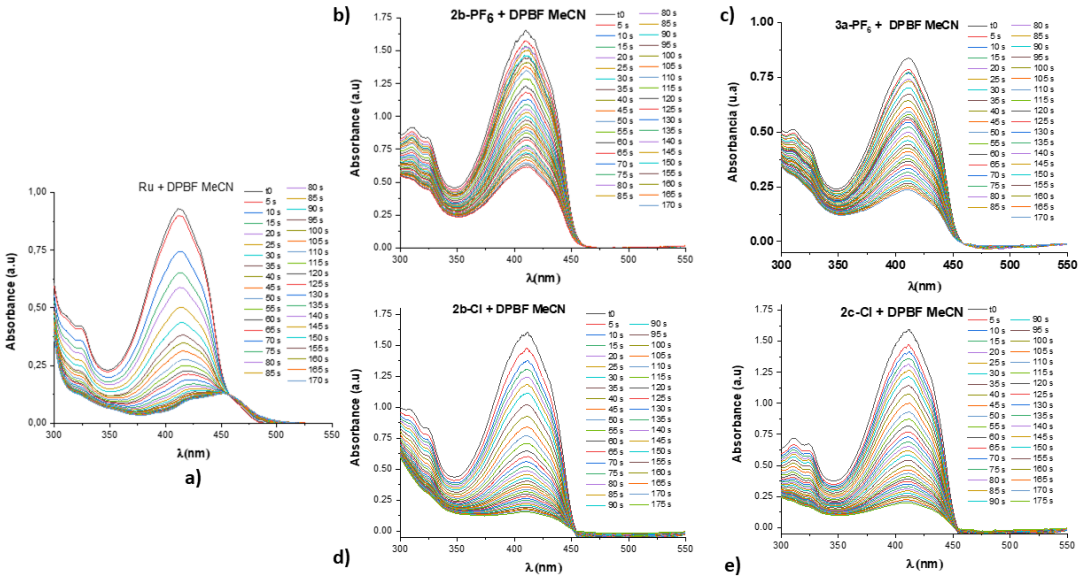

Figure S14. Changes in the absorbance measurements at 410 nm of the $^1O_2$ scavenger DPBF in acetonitrile solution in the presence of a) the reference $[Ru(bpy)_3]Cl_2$ b) **2b-PF$_6$** c) **3a-PF$_6$** d) **2b-Cl** and e) **2c-Cl**. ($\lambda_{irradiation}$ = 460 nm).

5.- Biological Studies

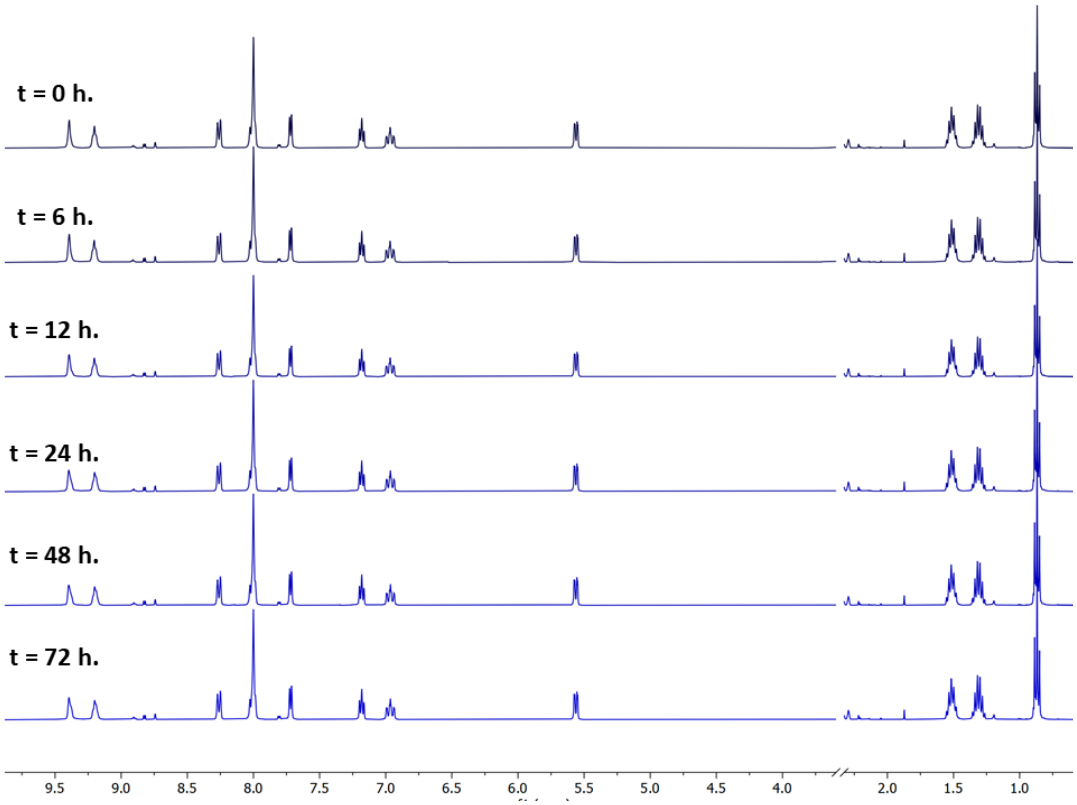

Figure S15. ^{1}H NMR spectra of **2a-Cl** in DMSO for 72 hours at 298 K.

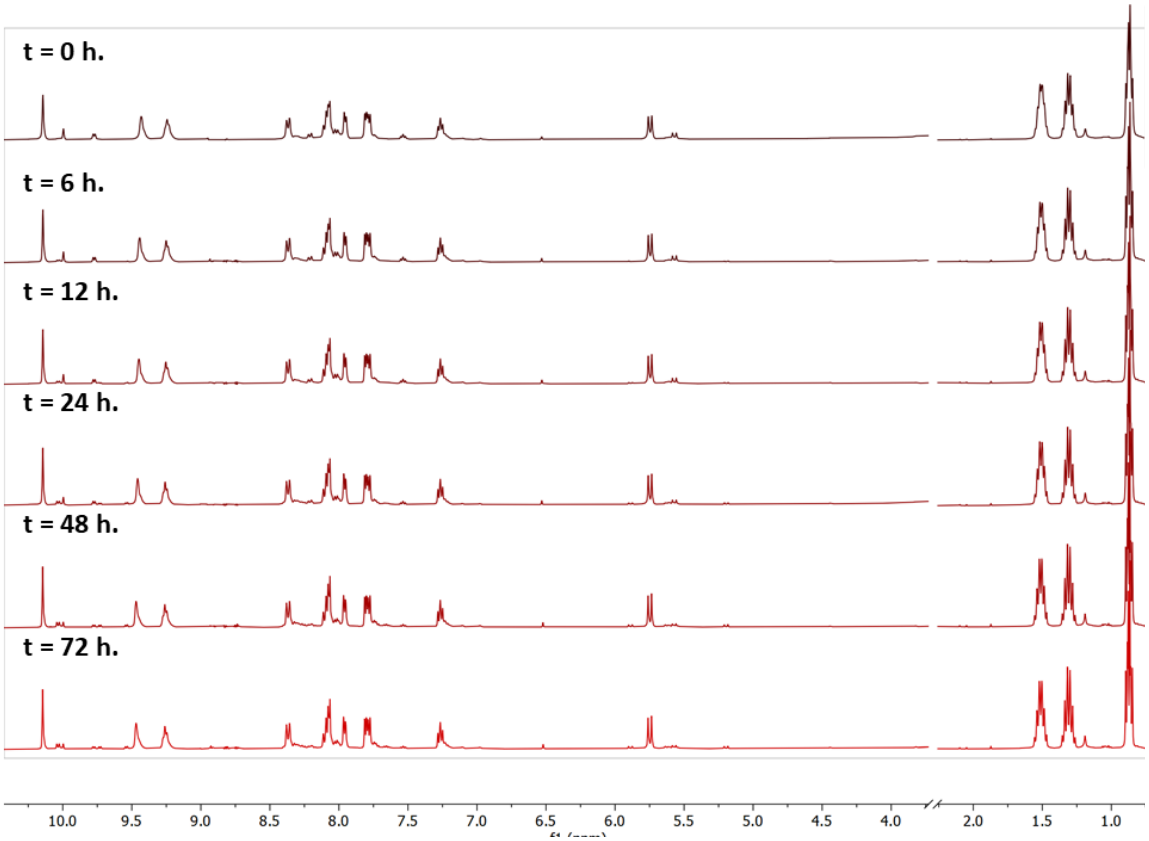

Figure S16. ^{1}H NMR spectra of **2b-Cl** in DMSO for 72 hours at 298 K.

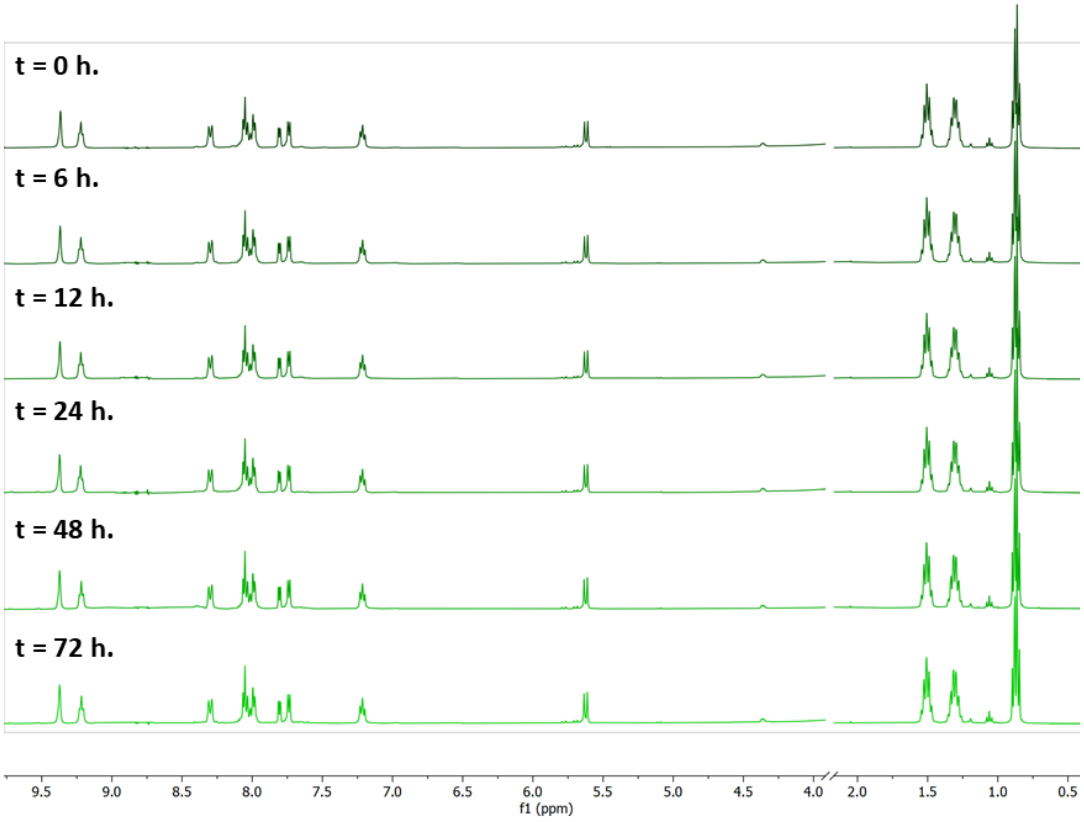

Figure S17. ^{1}H NMR spectra of **2c-Cl** in DMSO for 72 hours at 298 K.

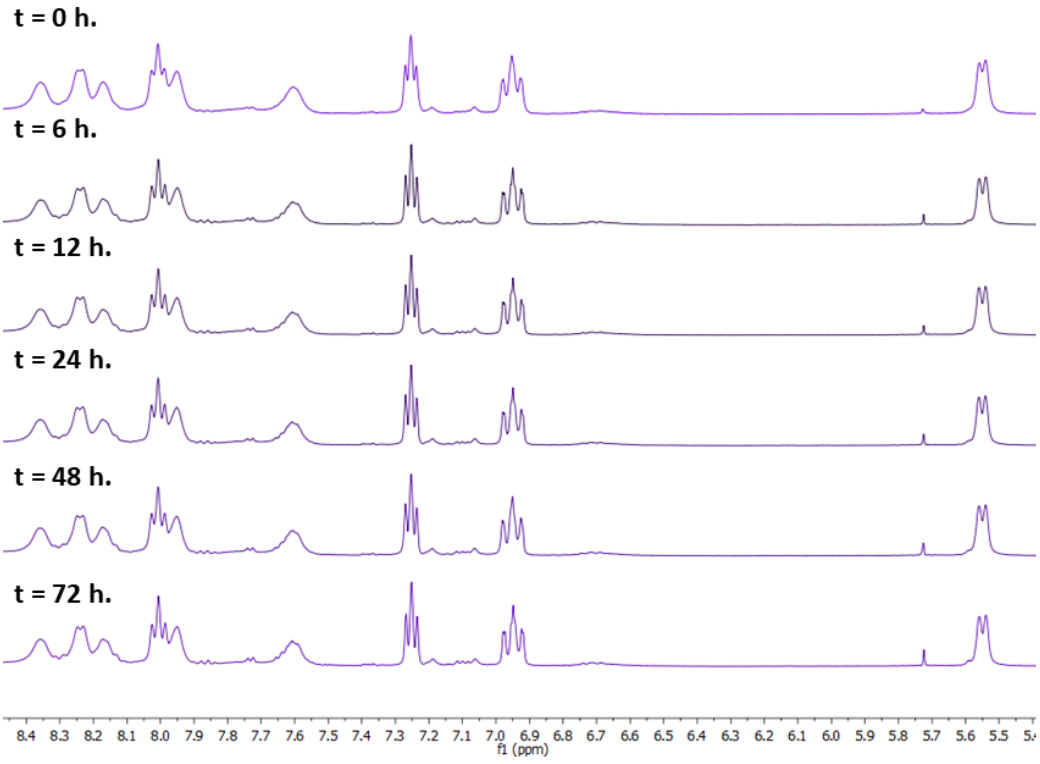

Figure S18: ^{1}H NMR spectra of **3a-PF$_6$** in DMSO for 72 hours at 298 K.

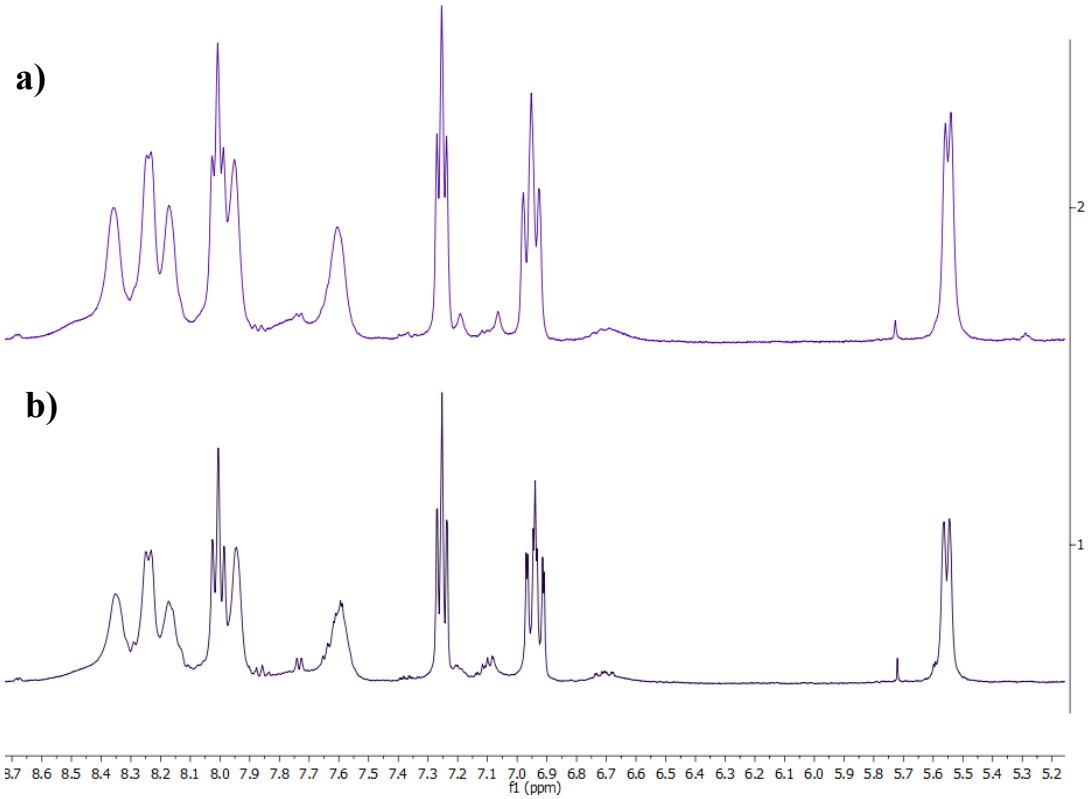

Figure S19. ^{1}H NMR spectra of **3a-PF$_6$** in DMSO (**a**) in dark conditions, (**b**) after 10 minutes of blue light irradiation (λ = 396 nm).

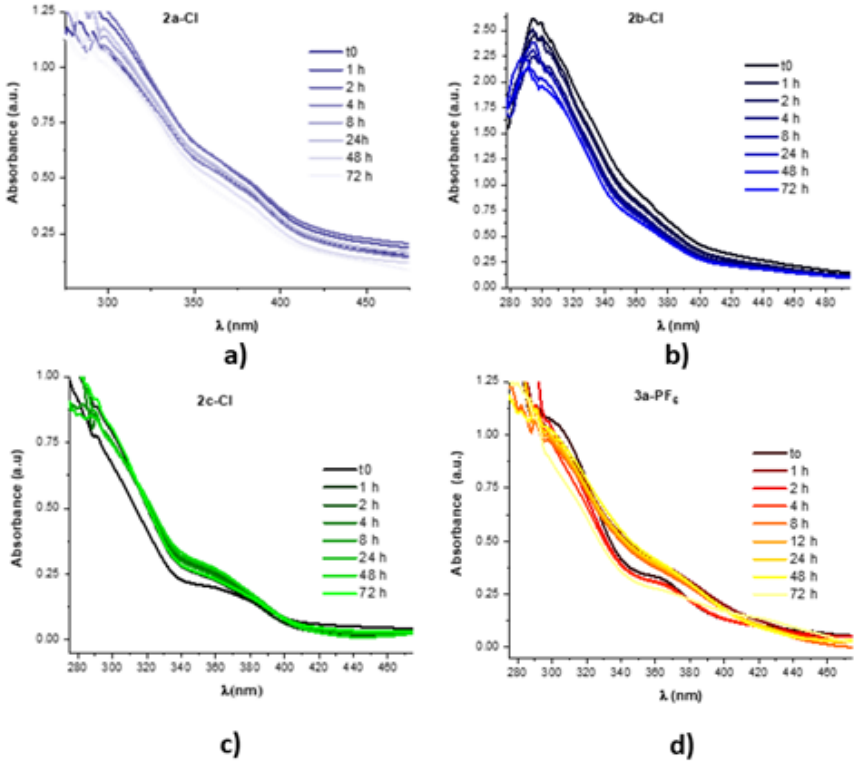

Figure S20. UV-vis absorption spectra of a) **2a-Cl**, b) **2b-Cl**, c) **2c-Cl** and d) **3a-PF$_6$** (5 x 10^{-5} M) recorded in DMSO (<1%)-cellular medium after been kept at room temperature since 0 h to 72 h (intervals in legends).

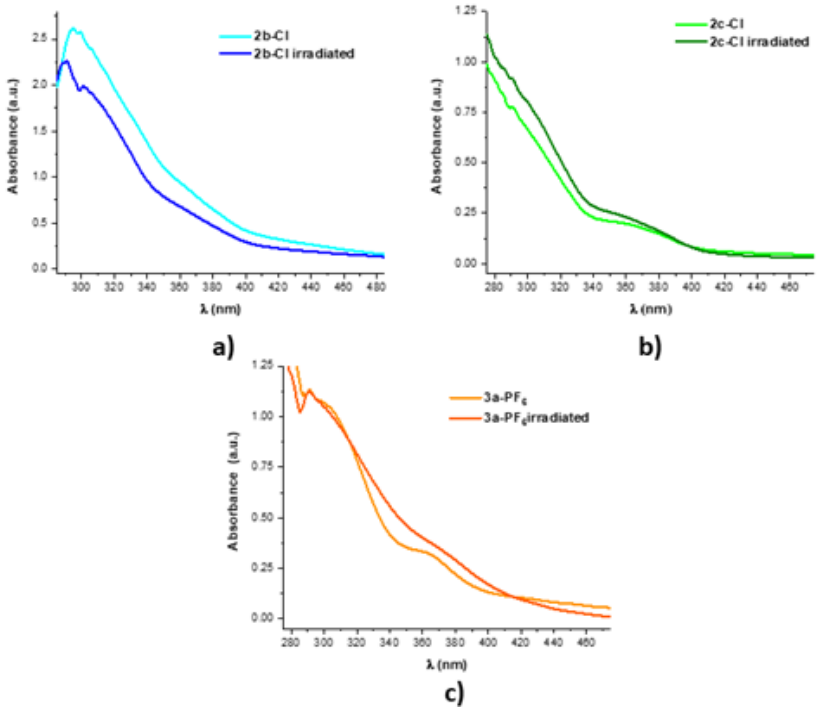

Figure S21. UV-vis absorption spectra of a) **2b-Cl**, b) **2c-Cl** and c) **3a-PF$_6$** (5 x 10^{-5} M) recorded in DMSO (<1%) - cellular medium before and after irradiation after 10 minutes of blue light irradiation (λ = 396 nm).

Cell lines and culture conditions

Two different human tumor cell lines: A549 (lung carcinoma) and HeLa (cervix carcinoma), as well as one nontumor human cell line BEAS-2B (bronchial epithelium), were cultured following the American Type Culture Collection (www.atcc.org) recommendations and standard methods, as previously described.[22, 23] Cells were maintained in RPMI 1640 with L-glutamine medium, supplemented with 10% fetal bovine serum (FBS), penicillin (100 U/mL) and streptomycin (100 µg/mL), kept under a humidified atmosphere of 95% air/5% CO_2 at 37°C, and sub-cultured before they get confluent using a 0.25% trypsin-EDTA solution.

Cytotoxicity Assay

The 3-(4,5-dimethylthiazol-2-yl)-5-(3-carboxymethoxyphenyl)-2-(4-sulfophenyl)-2H-tetrazolium (MTS) hydrolysis method (MTS-based CellTiter® 96. AQueous Assay; Promega Corp., Madison, WI) was used to determine the cell viability as an indicator of A549, HeLa and BEAS-2B cells sensitivity to the complexes as previously reported.[24] Briefly, 50 µL of exponentially growing cells were seeded at a density of $1.5x10^3$ (A549 and HeLa) and 6.0×10^3 (BEAS-2B) cells per well, in a 96-well flat-bottomed microplate in growing media, with reduced concentrations of FBS (5%) in case of A549. 24 h later, they were incubated for 72 h with the complexes that were dissolved in DMSO at 16 mM (**2c-Cl** and **3a-PF_6**) or 8 mM (**2a-Cl**, **2b** and **2c-PF_6**). Cisplatin (Alfa Aesar, Karlsruhe, Germany) as a reference was dissolved at 6.4 mM in a saline solution.[25] These stock solutions were kept frozen until they were dissolved in a test medium as nine 1:2 serial dilutions for the three cell lines. A total of 50 µL of each dilution or complete medium alone was added to growing cells in the 96-well plate designed as previously recommended.[26] Final concentrations in sextuplicates ranged from 400 to 1.56 µM (**2b-Cl**, **2b-PF_6**, **2c-PF_6** and **3a-PF_6**), from 200 to 0.78 µM (**2c-Cl**) and from 50 to 0.19 µM (**2a-Cl**) for A549 cells; from 400 to 1.56 µM (**3a-PF_6**), from 320 to 1.25 µM (**2b-PF_6**) and from 50 to 0.19 µM (**2a-Cl**) for HeLa cells; and from 400 to 1.56 µM (**2b-PF_6**, and **3a-PF_6**) and from 200 to 078 µM (**2a-Cl**) for BEAS-2B cells. In the case of cisplatin, serial dilutions were 1:1.5 ranging from 40 to 1.56 µM for A549 cells and 1:2 ranging from 200 to 0.78 µM for HeLa cells.[25] For BEAS-2B cells cisplatin serial dilutions were 1:2,5 ranging from 100 to 0,07 µM. After 72 h at 37 °C, 20 µL of MTS was added and plates were incubated for 1 h (A549 and HeLa) or 2 h (BEAS-2B) at 37 °C. Appropriate solvent controls were run along with samples to discard the DMSO cytotoxic effect. Final

concentrations of DMSO ranged from 0.63 to 0.002% (**2a-Cl**) for A549 and HeLa cells; from 1.5 to 0.005% (**2c-Cl**) for A549 cells; from 2.5 to 0.010% (**2a-Cl, 3a-PF_6**) for BEAS-2B cells, and (**3a-PF_6**) for A549 and HeLa cells; from 4 to 0.016% (**2b-PF_6**) for HeLa cells; and from 5 to 0.019% (**2b-Cl, 2b-PF_6, 2c-PF_6**) for A549 cells, (**2b-PF_6**) for BEAS-2B cells. In any case DMSO presence was found to interfere with complexes cytotoxicity determination. Finally, the optical density was measured at 490 nm using a 96-well multiscanner autoreader (POLARstar Omega; BMG Labtech, Offenburg, Germany). Each experiment was repeated three times. The IC_{50} (drug concentration that produced 50% inhibition of cell proliferation) was calculated by plotting the percentage of growing inhibition versus log of the drug concentration using the GraphPad Prism 6 (La Jolla, CA) software.

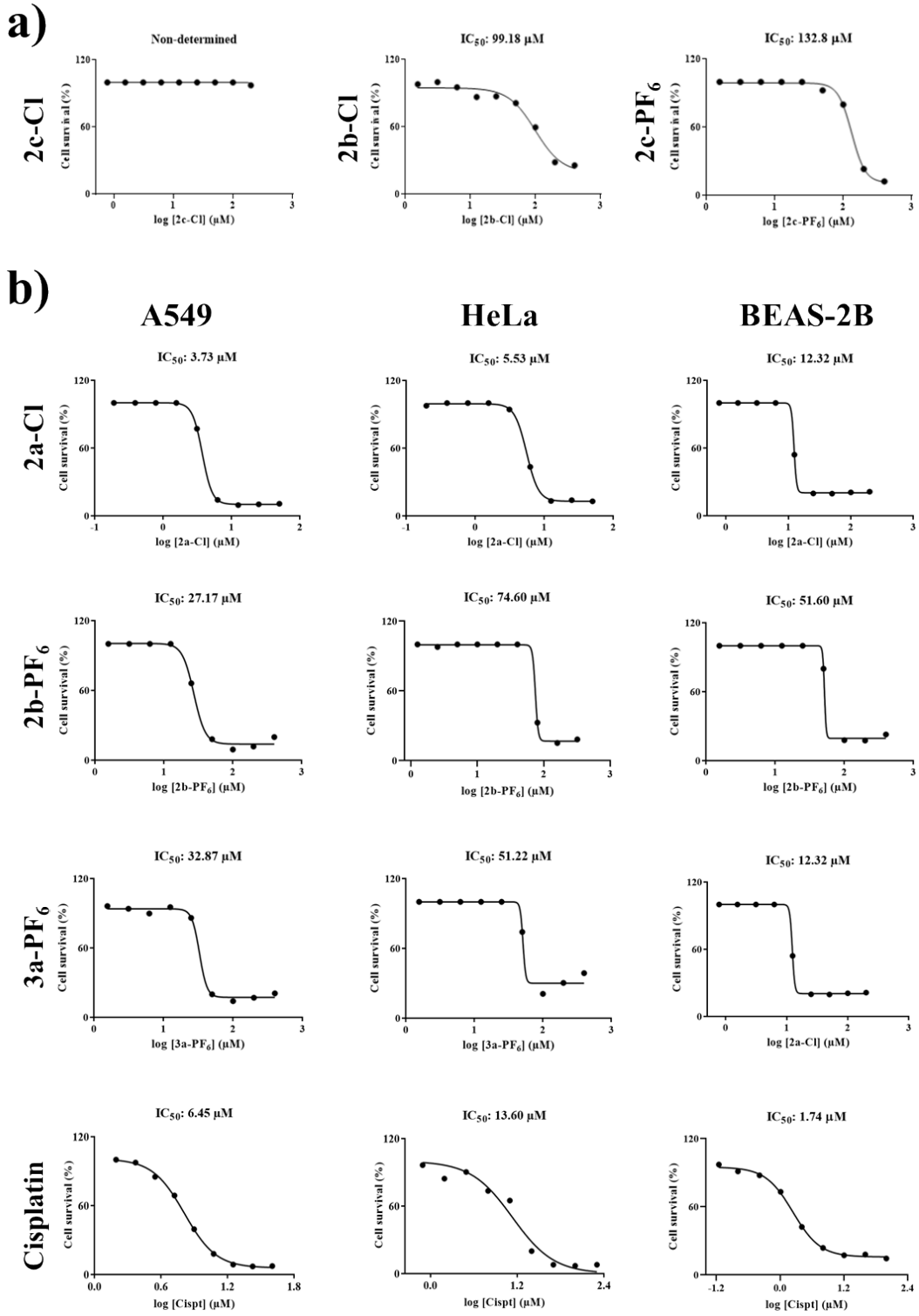

Figure S22. Dose-response curves for determination of the IC_{50} cytotoxicity values of all complexes tested and their comparison with cisplatin, in A549, HeLa and BEAS-2B cell lines. **a**) Graps with $IC_{50} \geq 100$ (**2b-Cl**: 99.8 µM, **2c-PF$_6$**: 132.8 µM) or with IC_{50} values that could not be determined (**2c-Cl**) in A549 cell line. **b**) IC_{50} values of **2a-Cl**, **2b-PF$_6$**, **3a-PF$_6$** complexes and cisplatin (CisPt) in A549, HeLa and BEAS-2B cell lines. The IC_{50} values correspond to the dose required to inhibit 50% cellular growth after cellular exposure to complexes for 72 h.

Selectivity index

The selectivity index (SI) was calculated according to the following equation: SI = IC_{50} non-tumor cell (BEAS-2B)/IC_{50} tumor cells (A549 or HeLa), as previously reported.[22] Nontumor BEAS-2B epithelial lung cells served as the selectivity reference to match the same tissue origin of A549 lung carcinoma (epithelial origin) cells, as suggested.[27]

***In vitro* Photocytotoxicity Testing**

Induction of phototoxicity in cultured cells was performed following previous reports, with modifications.[23] A549 cell were seeded in 96-well plates as described above for the MTS assay. 24 h later, cells were washed with HBSS (Hank's Balanced Salt Solution) (with 1 g/L glucose, without phenol red and pyruvate; Cat No. 14175-046 Gibco Thermo Fisher; Waltham, MA) and incubated in 50 µL sextuplicates of HBSS alone or in 1:2 nine serial dilutions in HBSS for 1 h at 37°C in a 5% CO_2 atmosphere. Final concentrations in sextuplicates ranged from 400 to 1.56 µM (**2b-PF_6**), from 200 to 0.78 µM (**2b-Cl** and **2c-Cl**) and from 150 to 0.59 µM (**3a-PF_6**). Final concentrations of DMSO ranged from 0.937 to 0.004% (**3a-PF_6**); from 1.5 to 0.005% (**2c-Cl**); from 2.5 to 0.010% (**2b-Cl**); and from 5 to 0.019% (**2b-PF_6**). In any case DMSO presence was found to interfere with complexes UV-cytotoxicity determinations. After 1 h of exposure to the complexes, plates were laid 91 mm under a LED lamp (λmax 396 nm; Onforu 15W IP66) and irradiated ("photoinduced" plate) under room normoxic atmosphere for 15 min (**2b-Cl** and **2c-Cl**), 10 min (**2b-PF_6**) and 3 min (**3a-PF_6**). Meanwhile, an equivalent control non-irradiated plate was manipulated in the same way ("nonphotoinduced" plate). After, cells were washed with HBSS, added 100 µL of complete medium and further incubated for 72 h at 37°C in a 5% CO2 atmosphere. Finally, 20 µL of MTS was added to each well, plates were incubated for 1 h at 37°C and the optical density was measured at 490 nm using a 96-well multi-scanner auto reader. Each experiment was repeated three times. The IC50 was calculated as described above under the Cytotoxicity Assay section.

Measurement of Reactive Oxygen Species (ROS)

The generation of ROS after UV irradiation of complexes was measured using a ROS-sensitive dye, 2',7'-dichlorodihydrofluorescein diacetate (H2DCFDA, Invitrogen, Carlsbad, CA, USA), as an indicator. Briefly, cells were seeded at 2x104 cells/well in 96-well plate containing 100 µL of culture medium. 24 h later, medium was removed and cells were incubated in 50 µL of HBSS-H2DCFDA (10 µM) without complexes (Control) or with different concentrations of complexes. Final concentrations were 1 and 25 µM

(**2b-Cl**); 2.25 and 25 μM (**2b-PF_6**); 1 and 50 μM (**2c-Cl**); and 1, 7 and 49 μM (**3a-PF_6**). These concentrations were chosen to be below and around or above the IC50 value after irradiation trying to avoid cytotoxic effects. After 1 h of exposure to the complexes, plates were laid 91 mm under a LED lamp (λ_{max} 396 nm; Onforu 15W IP66) and irradiated ("photoinduced" plate) under room normoxic atmosphere for 15 min (**2b-Cl** and **2c-Cl**), 10 min (**2b-PF_6**) and 3 min (**3a-PF_6**), the same times as those used for UV-IC50 determination. Each condition was performed in four wells (quadrupled replicates) on each plate. Meanwhile, an equivalent control non-irradiated plate was manipulated in the same way ("non UV" plate). Finally, 50 μL of HBSS was added to each well and the fluorescence intensity was monitored at 0, 15, 30, 45 and 60 min after irradiation at 485/535 nm (excitation/emission), using a microplate reader (Synergy 4; BioTek). Data presented correspond to 30 min after irradiation and were represented as obtained fluorescence intensity of exposed wells (arbitrary units). Each experiment was repeated three times.

Lipophilicity Determinations

Relative Lipophilicity measurements by RP-UPLC were performed using a Waters Acquity UPLC system (Waters, Milford, MA, USA), which was interfaced to quadrupole, high resolution, TOF mass spectrometer (micrOTOF-Q Bruker, Bremen, Germany), using an ESI interface operating in positive ion mode. The UPLC separation was performed using an Acquity UPLC BEH C18 1.7 μm particle size analytical column 100 mm × 2.1 mm (Waters) at a flow rate of 0.35 mL/min. The mobile phases used were A = H_2O with 0.1% HCOOH and B = acetonitrile with 0.1% HCOOH. The percentage of organic modifier (B) was changed linearly as follows: 0 min., 50%; 9.5 min., 99%; 11.5 min., 99%; 12 min., 20%; 12.5 min., 20%. Nitrogen (from a nitrogen generator) was used as the drying gas and nebulizing gas (2 Bar). The column temperature was set to 30°C. MS data were acquired over an m/z range of 50−3300. A capillary voltage of 4.5 kV, set end plate offset -500 V, dry gass of 7.0 L/min. and set dry heater of 190ºC were used. Calibrations were conducted from m/z 50 to 3300 with a HCOONa solution (15 mg) in 100 mL of water. MS data were acquired in centroid mode and were processed by the DataAnalysis application manager (within Compass Data Analysis 4.2 SR2; Bruker Corporation). Samples were dissolved in 10% v/v methanol in water, ∼10 μM.

Table S.9. Retention time (min.) of ionized picks of complexes.

Compound	Mass	Retention time (min.)
2a-Cl	**927.26**	**3.34**
2b-Cl	**983**	**1.93**
2b-PF_6	**983.25**	**1.87**
2c-Cl	**1015.18**	**1.20**
2c-PF_6	**1015.24**	**1.16**
3a-PF_6	**817.11**	**1.99**

Studio of reaction with NADH

The interaction between complexes **2a-Cl** and 3a (1 μM) with NADH (100 μM) in a solution of 20% Methanol and 80% H_2O was monitored by UV-Vis at 298 k after intervals of 1 hour. TON can be calculated as the difference in NADH concentration after 8 hours of reaction divided by the concentration of the complex being studied. The concentration of NADH was obtained employing the extinction coefficient ε_{339} = 6220 M^{-1} cm^{-1}.

Interaction of Complexes with DNA

The interaction between complexes and cisplatin with pBR322 plasmid DNA was studied by gel electrophoresis (mobility shift assay) as described by Frik *et al*.[28] The amount of DNA was kept constant (200 ng), while the concentrations of the compounds were varied to obtain increasing molar ratios with respect to plasmid DNA base pairs (0.5:1, 1:1, 2:1, 4:1 and 8:1). Aliquots of 2 μL of pBR322 plasmid DNA were mixed either alone or with 0.5, 1, 2, 4 or 8 μL of each compound solution (300 μM), respectively, in a 10 μL final volume of interaction buffer (50 mM NaClO4, 5 mM Tris-HCl, pH 7.5). Mixtures were incubated at 37 °C for 20 h in the dark and, after the addition of 2 μL of loading dye, were loaded onto 1% (w/v) agarose gels made in Trisacetate/ethylenediaminetetraacetic acid (EDTA) buffer (TAE) and separated by electrophoresis for 4 h at 70 V in TAE. Finally, gels were dyed for 30 min by immersion in a 3X solution of GelRed nucleic acid gel stain (Biotium Inc., Fremont, CA) diluted in 100 mM NaCl and images registered using a Gel-Doc System with the help of Quantity One software (BioRad, Hercules, CA).

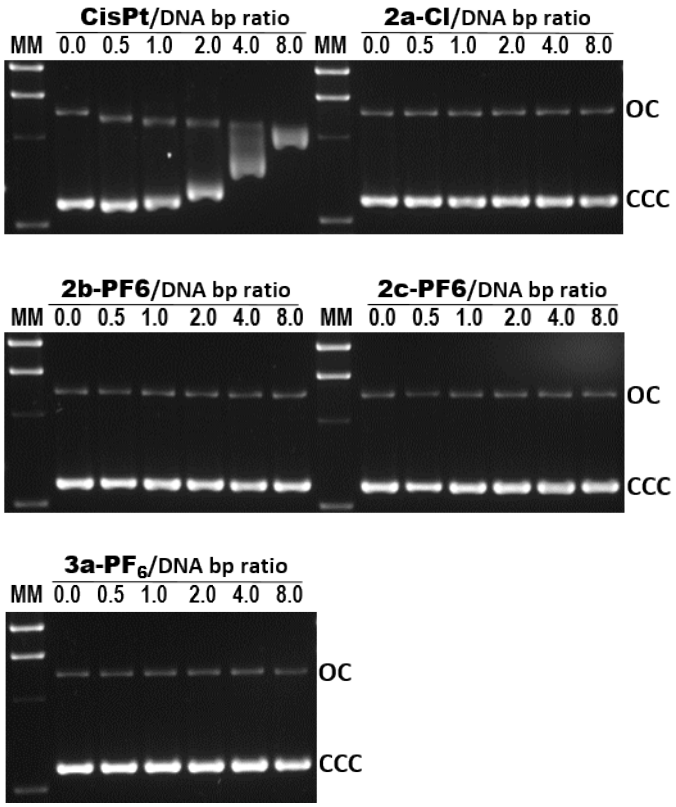

Figure S23. Electrophoresis mobility shift assay for cisplatin and compounds **2a-Cl**, **2b-PF_6**, **2c-PF_6** and **3a-PF_6**. CisPt, cisplatin; MM, λHindIII DNA molecular marker; Numbers refer to complex/plasmid DNA (pBR322); base pairs (bp) increasing ratios; OC, open circular (relaxed) plasmid DNA form; CCC, covalently closed circular (supercoiled) plasmid DNA form (as described in Ref. Millán *et al*.[22]

Cellular localization of complexes by confocal microscopy

Cytolocalization of compounds in living cells was analyzed as we previously described.[26]A549 cells were seeded onto poly-D-lysine-coated glass-bottomed culture dishes (MatTek Corporation, Ashland, MA) and let then grow up to 50-70 % confluency for 24-48 h. Next, the growth medium was removed and cells were incubated with different concentrations of compounds **2a-Cl**, **2b** (**Cl** and **PF_6**), **2c** (**Cl** and **PF_6**) and **3a-PF_6** in growth medium at 37°C in 5% CO_2 up to 24 h. To determine cytolocalization of compounds in nuclei, mitochondria or lysosomes, cells were co-stained with corresponding trackers: Hoechst 33342 (Sigma-Aldrich) and MitoTracker® Deep Red FM or LysoTracker® Red DND-99. To label mitochondria and lysosomes following treatments with compounds, media were removed and substituted with fresh media containing compounds and 3.2 μM Hoechst, 100 nM MitoTracker and/or 100 nM LysoTracker and incubated for 30 min at 37°C in 5% CO_2, in order to obtain either single or multiple fluorescent labelings.

Micrographs of living cells were taken at different incubation times with the compounds alone or combined with trackers using a Leica TCS SP5 laser scanning confocal. All images were taken at 37ºC and 5% CO_2 and using immersion oil. 405 Diode, Argon, and HeliumNeon (HeNe) laser lines were S8 applied to excite the samples and tunable filters were used to minimize crosstalk between fluorochromes. Gain, offset, and pinhole settings were identical for all samples within each experiment. The non-treated cells were used to establish the gain and offset settings to exclude non-specific and auto fluorescence. Images were documented with the help of LAS AF Lite microscopy software and projected into a single layer. The Fiji/ImageJ Open Source image processing software package was used to merge the single-layered images into one multilayered data set and to calculate the Pearson Correlation Coefficient.

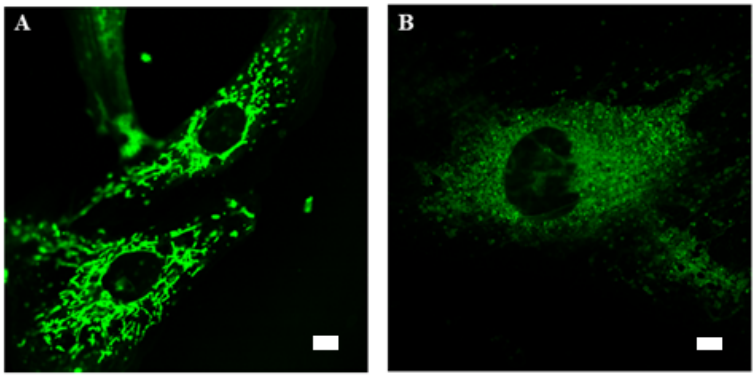

Figure S24: Laser confocal microscopy images of live fibroblasts stimulated with laser and labelled with MitoTracker (Green), **A**) incubated with complex **2a-Cl** at T = 0, **B**) incubated with complex **2a-Cl** at T = 1 hour. Scale bar = 10 μm.

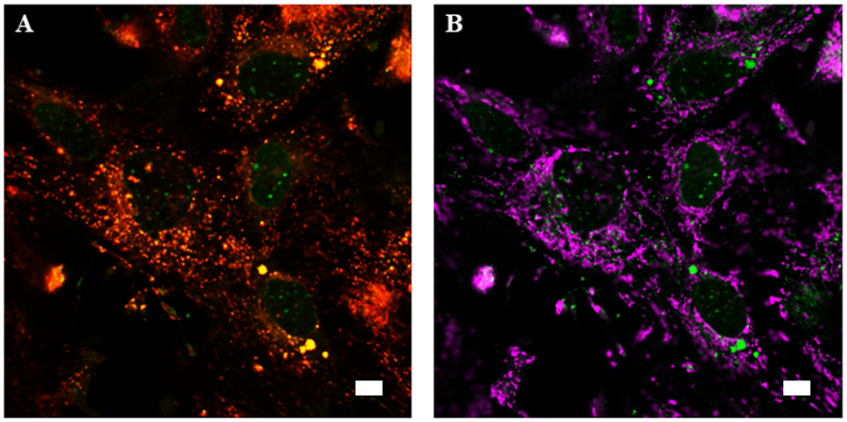

Figure S25: Laser confocal microscopy images of live fibroblasts stimulated with laser **A**) incubated with complex **2a-Cl** and labelled with LysoTracker, **B**) incubated with complex **2a-Cl** and labelled with MitoTracker. Red: LysoTracker; Magenta: MitoTracker; Green: complex **2a-Cl**. Scale bar = 10 μm.

Mitochondrial Membrane Potential Assay (MMP)

The MMP was measured using a JC-10 dye kit (Sigma Aldrich; ref. MAK159) following the manufacturer's instructions. Briefly, cells were seeded at $3x10^4$ cells/well in 96-well plates containing 90 µL of complete medium. 24 h later, 10 µL of complete medium without (Control) or with 16 µM **2a-Cl** complex were added to cells for 30 min. Each condition was performed in four wells (quadrupled replicates) on each plate. After, cells in wells that were incubated with **2a-Cl** were washed twice with PBS, and 100 µL of complete medium was added to them. Then, 50 µl of JC-10 dye in buffer A (1:100) was added to all wells and the plate incubated for 30 min. Finally, 50 µL of buffer B was added to each well and the fluorescence intensity was monitored at λ_{ex} = 490/ λ_{em} = 525 nm for green fluorescence and λ_{ex} = 540/ λ_{em} =590 nm for red fluorescence using a microplate reader (Synergy 4; BioTek) at 0, 10, 20 and 30 minutes. The ratio of red/green fluorescence intensity was used to determine MMP. Data presented correspond to 20 min and were represented as a percentage of MPP respect to control. In this experiment 10 mM of the uncoupler of oxidative phosphorylation (OXPHOS) in mitochondria, Carbonyl cyanide 4-(trifluoromethoxy)phenylhydrazone (FCCP) (Sigma Aldrich; ref. C2920), was used as positive control. Each experiment was repeated three times.

Statistical analysis

Following a Shapiro-Wilk normality test, the statistical significance was determined using Mann-Whitney U test or Student's *t*-test for comparing 2 groups. For all analysis, a p value < 0.05 was considered statistically significant. *$p < 0.05$; **$p < 0.01$; ***$p < 0.001$.

References for ESI

1. F. Lafolet, S. Welter, Z. Popović and L. De Cola, *J. Mater. Chem.*, 2005, **15**, 2820-2828.
2. N. Okamura, T. Nakamura, S. Yagi, T. Maeda, H. Nakazumi, H. Fujiwara and S. J. R. a. Koseki, *RSC Adv.*, 2016, **6**, 51435-51445.
3. A. Kimyonok, B. Domercq, A. Haldi, J.-Y. Cho, J. R. Carlise, X.-Y. Wang, L. E. Hayden, S. C. Jones, S. Barlow and S. R. J. C. o. M. Marder, *Chem. of materials*, 2007, **19**, 5602-5608.
4. C. Sahin, A. Goren, S. Demir and M. S. J. N. J. o. C. Cavus, *New. J. Chem.*, 2018, **42**, 2979-2988.
5. M. W. Cooke and G. S. Hanan, *Chem. Soc. Rev.*, 2007, **36**, 1466.
6. G. Sheldrick, *Acta Crystallogr. Sect. A*, 2015, **71**, 3-8.
7. G. M. Sheldrick, *Acta crystallogr., Sect. C*, 2015, **71**, 3-8.
8. L. J. Farrugia, *J. Appl. Crystallogr*, 1999, **32**, 837-838.
9. A. Spek, *J. Appl. crystallogr.*, 2003, **36**, 7-13.
10. A. L. Spek, *Acta Crystallogr. Sect. C Struct. Chem.*, 2015, **71**, 9-18.
11. M. J. Frisch, G. W. Trucks, H. B. Schlegel, G. E. Scuseria, M. A. Robb, J. R. Cheeseman, G. Scalmani, V. Barone, B. Mennucci, G. A. Petersson, H. Nakatsuji, M. Caricato, X. Li, H. P. Hratchian, A. F. Izmaylov, J. Bloino, G. Zheng, J. L. Sonnenberg, M. Hada, M. Ehara, K. Toyota, R. Fukuda, J. Hasegawa, M. Ishida, T. Nakajima, Y. Honda, O. Kitao, H. Nakai, T. Vreven, J. A. Montgomery, J. E. Peralta, F. Ogliaro, M. Bearpark, J. J. Heyd, E. Brothers, K. N. Kudin, V. N. Staroverov, R. Kobayashi, J. Normand, K. Raghavachari, A. Rendell, J. C. Burant, S. S. Iyengar, J. Tomasi, M. Cossi, N. Rega, J. M. Millam, M. Klene, J. E. Knox, J. B. Cross, V. Bakken, C. Adamo, J. Jaramillo, R. Gomperts, R. E. Stratmann, O. Yazyev, A. J. Austin, R. Cammi, C. Pomelli, J. W. Ochterski, R. L. Martin, K. Morokuma, V. G. Zakrzewski, G. A. Voth, P. Salvador, J. J. Dannenberg, S. Dapprich, A. D. Daniels, Farkas, J. B. Foresman, J. V. Ortiz, J. Cioslowski and D. J. Fox, *Gaussian 09, Revision B.01*, Gaussian, Inc., Wallingford CT, **2010**.
12. C. Lee, W. Yang and R. G. Parr, *Phys. Rev. B*, 1988, **37**, 785-789.
13. A. D. Becke, *Phys. Rev. A*, 1988, **38**, 3098-3100.
14. V. Barone and M. Cossi, *J. Phys. Chem. A*, 1998, **102**, 1995-2001.
15. N. M. O'Boyle, A. L. Tenderholt and K. M. Langner, *J. Comput. Chem.*, 2008, **29**, 839-845.
16. T. Lu and F. Chen, *J. Comput. Chem.*, 2012, **33**, 580-592.
17. W. Humphrey, A. Dalke and K. Schulten, *J. Mol. Graph.*, 1996, **14**, 33-38.
18. N. Adarsh, R. R. Avirah and D. Ramaiah, *Org. Lett.*, 2010, **12**, 5720-5723.
19. P. Majumdar, X. Yuan, S. Li, B. Le Guennic, J. Ma, C. Zhang, D. Jacquemin and J. Zhao, *J. Mat. Chem. B*, 2014, **2**, 2838-2854.
20. S. P.-Y. Li, C. T.-S. Lau, M.-W. Louie, Y.-W. Lam, S. H. Cheng and K. K.-W. Lo, *Biomaterials*, 2013, **34**, 7519-7532.
21. Y. Lu, R. Conway-Kenny, J. Wang, X. Cui, J. Zhao and S. M. Draper, *Dalton Trans.*, 2018, **47**, 8585-8589.
22. G. Millan, N. Gimenez, R. Lara, J. R. Berenguer, M. T. Moreno, E. Lalinde, E. Alfaro-Arnedo, I. P. Lopez, S. Pineiro-Hermida and J. G. Pichel, *Inorg. Chem.*, 2019, **58**, 1657-1673.
23. R. Lara, G. Millan, M. T. Moreno, E. Lalinde, E. Alfaro-Arnedo, I. P. Lopez, I. M. Larrayoz and J. G. Pichel, *Chem. Eur. J.*, 2021, **27**, 15757-15772.

24. J. R. Berenguer, J. G. Pichel, N. Gimenez, E. Lalinde, M. T. Moreno and S. Pineiro-Hermida, *Dalton Trans.*, 2015, **44**, 18839-18855.
25. E. Lalinde, R. Lara, I. P. Lopez, M. T. Moreno, E. Alfaro-Arnedo, J. G. Pichel and S. Pineiro-Hermida, *Chem. Eur. J.*, 2018, **24**, 2440-2456.
26. OECD, *OECD Series Test Assess*, 2010, **20**, 1-54.
27. M. López-Lázaro, *Oncoscience*, 2015, **2**, 91.
28. M. Frik, J. Jiménez, V. Vasilevski, M. Carreira, A. De Almeida, E. Gascón, F. Benoit, M. Sanaú, A. Casini and M. Contel, *Inorg. Chem. Front.*, 2014, **1**, 231-241.